PCCP

ROYAL SOCIETY OF CHEMISTRY

PERSPECTIVE

View Article Online
View Journal | View Issue

Cite this: *Phys. Chem. Chem. Phys.*, 2021, **23**, 785

Deep eutectic solvents as non-traditionally multifunctional media for the desulfurization process of fuel oil

Zhiguo Zhu,[a] Hongying Lü,*[a] Ming Zhang[b] and Hengquan Yang*[b]

Deep eutectic solvents (DESs) have been intensively pursued in the field of separation processes, catalytic reactions, polymers, nanomaterial science, and sensing technologies due to their unique features such as the low cost of components, ease of preparation, tunable physicochemical properties, negligible vapor pressure, non-toxicity, renewability, and biodegradability in the recent decade. Considering these appealing merits, DESs are widely used as extraction agents, solvents and/or catalysts in the desulfurization process since 2013. This review is focused on summarizing the physicochemical properties of DESs (*i.e.*, freezing point, density, viscosity, ionic conductivity, acidity, hydrophilicity/hydrophobicity, polarity, surface tension, and diffusion) to some extent, and their significant advances in applications related to desulfurization processes such as extraction desulfurization, extraction–oxidation desulfurization, and biomimetic desulfurization. In particular, we systematically compile very recent works concerning the selective aerobic oxidation desulfurization (AODS) under extremely mild conditions (60 °C and ambient pressure) *via* a biomimetic approach coupling DESs with polyoxometallates (POMs). In this system, DESs act as multifunctional roles such as extraction agents, solvents, and catalysts, while POMs serve as electron transfer mediators. This strategy is inspirational since biomimetic or bioinspired catalysis is the "Holy Grail" of oxidation catalysis, which overcomes the difficulty of O_2 activation *via* introducing electron transfer mediators into this system. It not only can be used for AODS, but also paves a novel way for oxidation catalysis, such as the selective oxyfunctionalization of hydrocarbon. Eventually, the conclusion, current challenges, and future opportunities are discussed. The aim is to provide necessary guidance for precisely designing tailor-made DESs, and to inspire chemists to use DESs as a powerful platform in the field of catalysis science.

Received 30th September 2020,
Accepted 8th December 2020

DOI: 10.1039/d0cp05153e

rsc.li/pccp

1. Introduction

Sulfur oxide (SO_x) exhausted from the combustion of fossil fuels such as coal, gasoline, and diesel, which causes irreversible damage to human health and environmental systems has brought about intense concern all around the world.[1–3] Prolonged exposure to SO_x poses a great threat to lungs, skin, eyes, and even the respiratory system of the human body.[3,4] Moreover, SO_x is one of the main sources of environmental pollution, such as acid rain and haze.[5,6] The combustion of fuel oil containing organic sulfide in automotive engine was the largest contributor except for SO_x emission from the process of electricity generation using coal as an energy provider.[7] Sulfur in fuel oil (mainly gasoline and diesel) generally exists in the form of organic species, such as mercaptan, thioether, disulphide, thiophene, and benzothiophene derivatives, as shown in Fig. 1. Therefore, many national governments have put forward more and more stringent regulations to decrease sulfur contents in fuel oil.

At present, the criterion of sulfur content is mainly classified into American, European, Japanese, and Chinese systems. In 2010, the American government required the sulfur content to be as low as 15 ppm. In Japan, the lower sulfur content of 10 ppm was the norm since 2008. The European Union has implemented Euro VI fuel standard for fuel with 10 ppm as of 2014. China has enacted the National V fuel standard, which has an allowable sulfur content below 10 ppm since 2017.[7,8] It is highly desired to obtain fuel oil with low, even free, sulfur contents. In this context, desulfurization technology is of ever-increasing importance. The current desulfurization technology mainly comprises hydrodesulfurization (HDS) and non-hydrodesulfurization technologies. HDS is widely and maturely adopted in the desulfurization process because of its high efficiency in removing aliphatic organosulfur compounds.[9]

[a] *Green Chemistry Centre, College of Chemistry and Chemical Engineering, Yantai University, 30 Qingquan Road, Yantai 264005, Shandong, China. E-mail: hylv@ytu.edu.cn*
[b] *School of Chemistry and Chemical Engineering, Shanxi University, Taiyuan 030006, China. E-mail: hqyang@sxu.edu.cn*

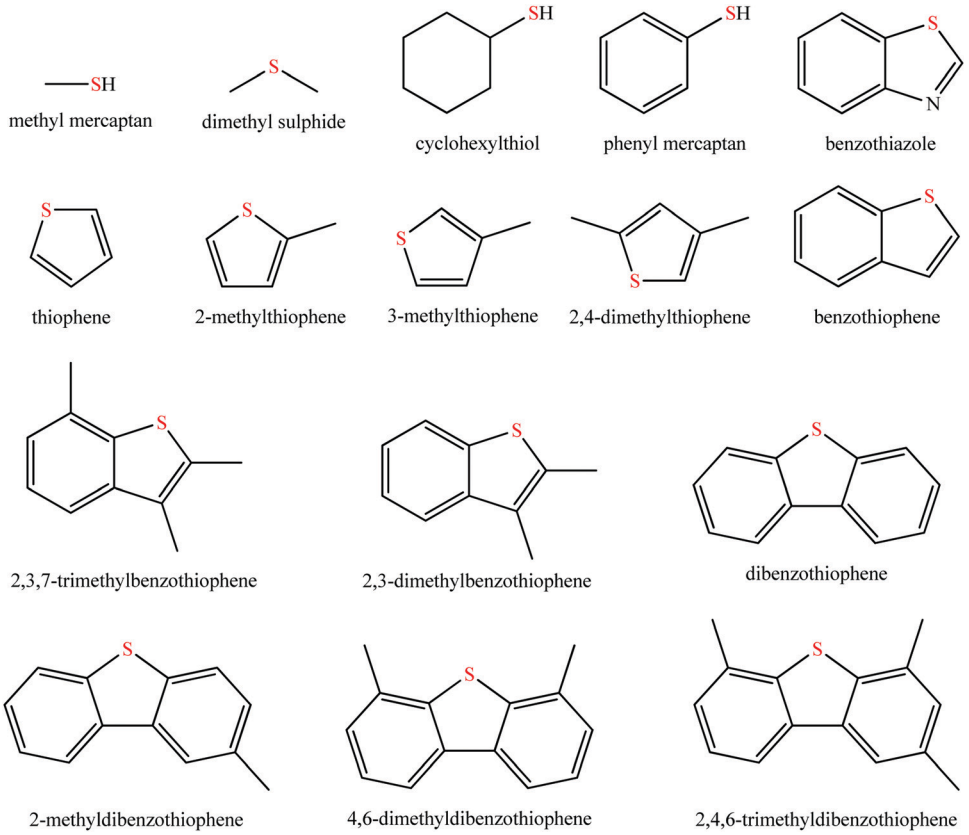

Fig. 1 Possible organic sulfur compounds in the fuel oil.

However, some drawbacks have gradually become pronounced, such as environmentally-unfriendly conditions (temperature, 300–400 °C; pressure, 2–10 MPa) and employing high-cost noble metal catalysts.[9,10] Additionally, these organic sulfides consisting of benzothiophene (BT), dibenzothiophene (DBT), 4,6-dimethyldibenzothiophene (4,6-DMDBT), and their derivatives are hardly eliminated by HDS due to the stable C–S conjugated system in the thiophene ring and/or steric hindrance.[11] Furthermore, the C=C bond in olefins is likely saturated *via* hydrogenation, giving rise to the decrease of the octane number for gasoline.[12] Considering these issues associated with HDS, the adsorptive desulfurization,[8] extractive desulfurization,[13] and oxidative desulfurization[14] are thus born as alternative technologies. The common adsorbents include metal oxide,[15] metal ion-exchanged zeolite,[16,17] and activated carbon.[8] With respect to extractive desulfurization, the conventional extraction agents are mainly polar organic solvents, including furfural, tetramethylene sulfone, *N*-methylpyrrolidone, dimethyl sulfoxide, acetonitrile, and others.[18] In spite of possessing merits of relatively mild operation conditions, low expense, and resisting the loss of the octane number for gasoline, this desulfurization strategy is still problematic because of the poor selectivity of extraction agents to discrepant sulfides and the great energy consumption for their recovery.[13,18]

Ionic liquids (ILs) as solvents for extraction desulfurization have received significant attention in the past 20 years, which has been systematically reviewed.[13] ILs are generally formed *via* ionic bonds and exist in the molten state, whose physicochemical property can be tailored by altering the anions and/or cations.[19] Nonetheless, the high-cost and inferior biodegradability are the dominating concerns for ILs in light of sustainable development and environmental protection.[20] It is of significance for extraction desulfurization to develop an alternative to replace the current ILs.

Deep eutectic solvents (DESs), a new class of solvents, emerged in 2003.[21] Their physicochemical properties (*e.g.*, density, conductivity, surface tension, viscosity) are similar to these of ILs.[22] However, DESs have many merits such as ease of preparation *via* the simple mixing of some organics, their low price, biodegradation, biocompatibility, and non-toxicity (Fig. 2), which are virtually unachievable for traditional ILs.[22–25] Owing to these features, DESs are intensively studied at both academic and industrial levels, including our group. In the past 5 years, the reviews about the application of DESs in the desulfurization process mainly focus on the extraction desulfurization.[7,26,27] Only one review concerning the application of liquid/liquid biphasic oxidations with ILs or DESs, involves the partial description of the oxidative desulfurization process using hydrogen peroxide as an oxidant.[28] These existing reviews cannot keep pace with the expeditious utilization of DESs in oxidative desulfurization (ODS), especially for aerobic oxidative desulfurization (AODS) in the recent decade. Such an ever-expanding gap motivates us to review the cutting-edge advances, discuss the current challenges and future opportunities. This review is focused on summarizing the physicochemical properties of DESs and their applications in the desulfurization process.

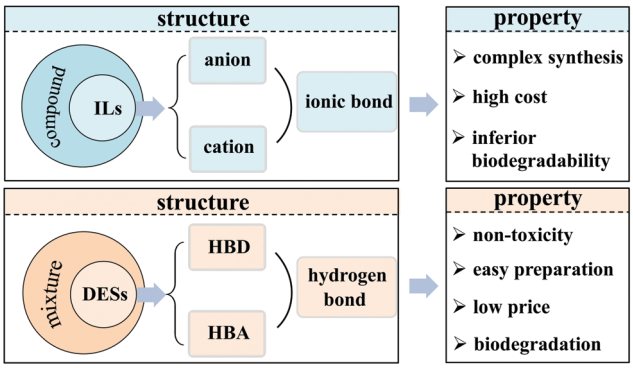

Fig. 2 The comparison of the structure and property between ionic liquids (ILs) and deep eutectic solvents (DESs). HBD and HBA indicate hydrogen bond donor and hydrogen bond acceptor, respectively.

2. Definition of DESs

DESs, also called deep eutectic ionic liquids (DEILs) or low-melting mixtures (LMMs) or low transition temperature mixtures (LTTMs) in the literature,[23,29] are made up of more than two components, which interact with each other *via* hydrogen bonds. The melting point of the resultant DESs is lower than that of each individual component.[24,25] It is worthwhile mentioning that most of them exist in the liquid phase from room temperature to 80 °C.[30] In most cases, DESs are prepared by simply mixing a hydrogen bond donor (HBD) and hydrogen bond acceptor (HBA).[23–25,29–31] The HBA and HBD are generally a quaternary ammonium or phosphonium salt and organic acid or alcohol, respectively, as summarized in Fig. 3. The physicochemical properties of DESs can be tailored at will by choosing suitable HBD and HBA, and/or by adjusting their molar ratio.

DESs are commonly divided into four types, depending on the nature of the raw materials: type I, $Q^+X^-{\cdot}zMCl_x$, M = Zn, Sn, Fe, Ga, Al; type II, $Q^+X^-{\cdot}zMCl_x{\cdot}yH_2O$, M = Cr, Fe, Cu, Ni, Co; type III, $Q^+X^-{\cdot}zRZ$, Z = $-CONH_2$, $-COOH$, $-OH$; type IV, $MCl_x{\cdot}RZ$, M = Al and Zn, Z = $-CONH_2$, $-OH$. Q, X, and R are generally a quaternary ammonium (or quaternary phosphonium), halide anion, and alkyl group, respectively.[25,32] Obviously, types I, II, and IV can generate Lewis acid DESs, while Brønsted acid DESs can be derived from type III.[7,32,33] It should be noted that choline chloride (ChCl) is often chosen as HBA, taking account of its low cost and environmental friendliness (biodegradability, biocompatibility, and low toxicity). Numerous DESs can be formed using ChCl and HBD, such as urea, renewable carboxylic acid (oxalic acid, citric acid, amino acid), and polyhydric alcohols (polyethylene glycol, glycerine, saccharides).[22,25,33,34] It is notable that the starting materials of DESs can be a non-ionic compound, which is different from ILs. The Abbott group synthesized a DES from solid ChCl and urea, whose melting point was as low as 12 °C.[21] Namely, this DES exists in the liquid phase at room temperature. DESs are not definitely confined to two compounds, and a ternary DES was task-specifically designed from boric acid, 1-butyl-3-methylimida-zolium chloride, and glutaric acid for the transformation of CO_2 into cyclic carbonates.[35]

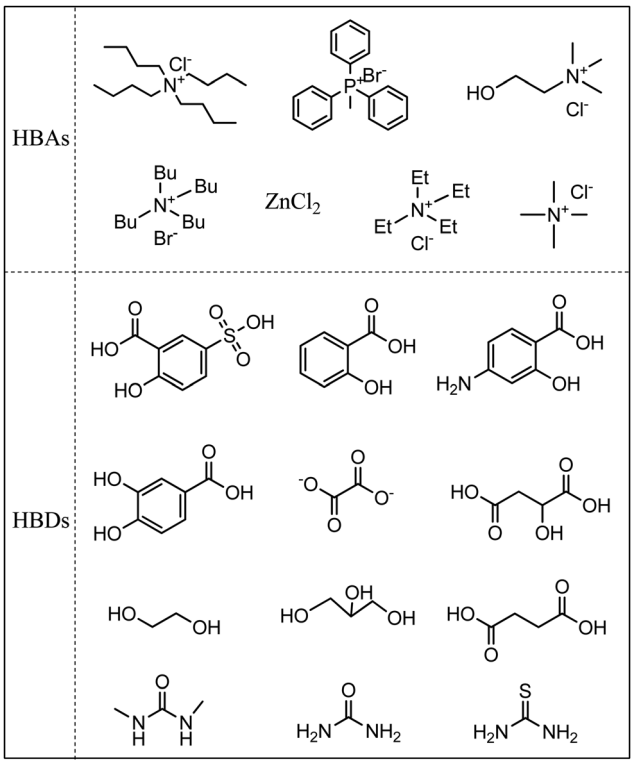

Fig. 3 Representative structures of HBAs and HBDs for the preparation of DESs.

3. Physicochemical properties of DESs

The physicochemical properties of DESs are closely related to their practical applications. DESs demonstrate not only the features of low vapor pressure, strong dissolving capacity, and ease of storage like conventional ILs, but also unique characterizations in terms of the freezing point, density, viscosity, ionic conductivity, acidity, hydrophilicity/hydrophobicity, polarity, surface tension, and diffusion.

3.1. Freezing point (T_f)

One distinctive feature of DESs is the T_f being lower than each individual constituent. For instance, the T_f (−30 °C) of DES derived from glycol and $ZnCl_2$ with the corresponding molar ratio of 4 was inferior to that of either glycol (−12.9 °C) or $ZnCl_2$ (290 °C), which may be due to the hydrogen bond interaction.[36] DESs with T_f below 50 °C are attractive from the viewpoint of practical applications in the field of separation processes, catalytic reactions, polymer, nanomaterial science, and sensing technologies.

The molar ratio of HBA to HBD and their nature have great impacts on the T_f of DESs. For example, DESs prepared from urea and ChCl with the molar ratio of 1 : 1 and 2 : 1 demonstrated a T_f of about 53 °C and 12 °C, respectively.[21] When ChCl was mixed with $FeCl_3$ and $SnCl_2$ using the same molar ratio of 1 : 2, the obtained DES showed a T_f of 65 and 37 °C, respectively.[37] The anion of HBA also affects the T_f of the generated DESs. For instance, the T_f of choline salt-based DESs

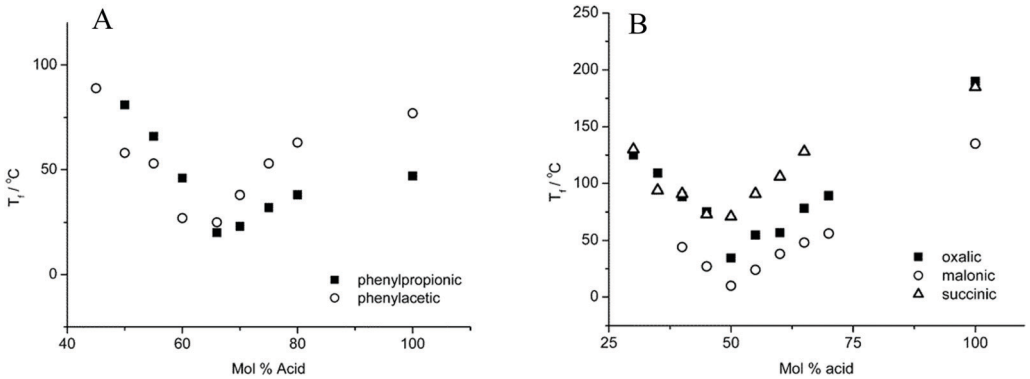

Fig. 4 Freezing points of five choline chloride-based DESs as a function of the composition. Reprinted with permission from ref. 22. Copyright (2004) American Chemical Society.

using urea as HBD followed the sequence of $T_f(F^-) > T_f(NO_3^-) > T_f(Cl^-) > T_f(BF_4^-)$, in agreement with the strength of the hydrogen bond.[21]

The molar ratio of HBA to HBD for the lowest T_f of various DESs is greatly discrepant.[22,38] As shown in Fig. 4, the lowest T_f for phenylpropionic acid and phenylacetic acid-based DESs with ChCl was achieved at a composition of 67 mol% of HBD, whereas that for diacid was generated with 50 mol% of HBD. This experiment phenomenon indicated that two carboxylic acid functional groups interacted with one ChCl. Moreover, matching the melting point for each individual component is the key point to form a DES.[39]

3.2. Density

Density (ρ) is a basic and significant factor for DESs, which can determine some factors, such as the thermal expansion coefficient (α), molecular volume (V_m), and lattice energy (U_{POT}) based on the following equation.[40,41] The α and U_{POT} values are closely associated with the free volume and strength of interactions between ions.

$$\ln \rho = b - \alpha \cdot T, \quad V_m = M/(N \cdot \rho), \quad U_{POT} = 1981.2 \cdot (\rho/M)^{1/3} + 103.8$$

The density values of common DESs are exhibited in Table 1.[42–49] Obviously, their density values are in the region of 1.10 to 1.63 g cm^{-3} at 25 °C, which are higher than that for water.

Table 1 Physicochemical properties of various DESs at 25 °C[a]

No.	HBA	HBD	HBA : HBD (mol : mol)	Density (g cm^{-3})	Viscosity (cP)	Conductivity (mS cm^{-1})	Ref.
1	ChCl	Glycerol	1 : 1	1.16	N/A[b]	N/A	42
2	ChCl	Glycerol	1 : 3	1.20	N/A	N/A	42
3	$ZnCl_2$	Urea	1 : 3.5	1.63	11340	0.18 (40 °C)	32
4	$ZnCl_2$	Acetamide	1 : 4	1.36	N/A	N/A	32
5	$ZnCl_2$	EG	1 : 4	1.45	N/A	N/A	32
6	$ZnCl_2$	Hexanediol	1 : 3	1.38	N/A	N/A	32
7	BTEC	PTSA	3 : 7	1.17	12698	0.041	43
8	BTEC	Oxalic acid	1 : 1	1.17	41080	1.21	43
9	BTEC	Citric acid	1 : 1	N/A	N/A	0.002	43
10	$FeCl_3{\cdot}6H_2O$	EG	2 : 1	1.61	43.37	45.4	44
11	$FeCl_3{\cdot}6H_2O$	Glycerol	3 : 1	1.64	99.16	26.8	44
12	$FeCl_3{\cdot}6H_2O$	Malonic acid	2 : 1	1.62	33.16	108.3	44
13	$FeCl_3{\cdot}6H_2O$	PT	2 : 1	1.62	33.16	108.3	44
14	$FeCl_3{\cdot}6H_2O$	Xylitol	2 : 1	1.63	446.54	10.1	44
15	$FeCl_3{\cdot}6H_2O$	Serine	2 : 1	1.67	380.89	19.4	44
16	$FeCl_3{\cdot}6H_2O$	Alanine	2 : 1	1.63	119.75	37.4	44
17	$FeCl_3{\cdot}6H_2O$	Glycine	2 : 1	1.68	156.62	43.9	44
18	ChCl	Malonic acid	1 : 2	1.25	721.0	0.55	22
19	ChCl	PTSA	1 : 2	1.24	697.9	0.62	45
20	ChCl	TA	1 : 2	1.46	434.99	0.071	45
21	ChCl	MA	1 : 2	1.28	117.93	0.32	45
22	ChCl	PA	1 : 2	1.08	55.91	0.39	45
23	$EtNH_3Cl$	CF_3CONH_2	1 : 1.5	1.273	256.0	0.39	46
24[c]	ChCl	CF_3CONH_2	1 : 2	1.342	77.0	0.286	46
25[d]	PEG	OXA	1 : 2	N/A[a]	381.0	2.0	47
26[d]	Bu_4NBr	Imidazole	3 : 7	N/A[a]	44.0	3.0	48
27[d]	PEG	BSA	2.5 : 1	N/A[a]	190.2	24.3	49

[a] Abbreviations: ethylene glycol, EG; benzyltriethylammonium chloride, BTEAC; *p*-toluenesulfonic acid, PTSA; pentaerythritol, PT; trichloroacetic acid, TA; monochloroacetic acid, MA; propionic acid, PA; polyethylene glycol 2000, PEG; oxalate dehydrate, OXA; benzenesulfonic acid, BSA. [b] Indicating not available. [c] Measured at 40 °C. [d] Measured at 60 °C.

Besides, both the composition and molar ratio of HBA to HBD influence the density of the formed DES, just like the freezing point (ChCl : glycerol = 1 : 1, 1.16 g cm^{-3} *versus* ChCl : glycerol = 1 : 3, 1.20 g cm^{-3}).[42] It is noted that the density value of DESs exceed the HBD individual (DES ($ZnCl_2$: acetamide = 1 : 4), 1.36 g cm^{-3} *versus* acetamide, 1.16 g cm^{-3}), which may be due to the hole theory.[29] The following equation can be used to roughly predict the density of DESs.[50]

$$\rho = \left(0.01256 + \frac{0.9533M}{V_c}\right)\left[\left(\frac{0.0039}{M}2 + \frac{0.2987}{V_c}\right)V_c^{1.033}\right]^{\psi}$$

$$\psi = -\left[\frac{1 - T_r}{1 - T_{br}}\right]^{\frac{2}{7}}$$

V_c, M, T_r, and T_{br} are the critical volume, molecular mass, reduced temperature, and normal boiling point, respectively.

3.3. Viscosity

The viscosity of DESs (one kind of fluid) is equal to the shearing force facilitating the fluid flow per velocity gradient in the moving direction, which can reflect the mobility of free species, such as cations and anions within DESs.[51] As for DESs, a low viscosity is urgently expected in practical chemical applications as green solvents, in favor of mass and momentum transfer.[46] Unfortunately, most of the DESs have high viscosity values greater than 100 cP, as shown in Table 1. The high viscosity may result from the strong hydrogen bond network. That is, the presence of a hydrogen bond is a double-edged sword in that it promotes the formation of DESs and at the same time, also increases their viscosity.

Additionally, the viscosity of DESs is generally related to the nature of HBA and HBD, the molar ratio of HBA to HBD, the temperature, and the water amounts.[25] For instance, with the increase of the ChCl/glycerol molar ratio and temperature, the viscosity of the ChCl/glycerol DES decreased (Fig. 5).[52] This can be explained by the partial rupture of the intermolecular hydrogen bond for glycerol with the addition of ChCl. Polyethylene glycol (PEG) was mixed with one of an organic acid containing 3,4-dihydroxybenzoic acid (DHBA), 5-sulfosalicylic acid (SSA), salicylic acid (SA), oxalate dihydrate (OXA), *p*-amino salicylic acid (PAS), and DL-malic acid (DL-MA), which were chosen as the HBD to generate the corresponding DES.[47] As illustrated in Fig. 5, PEG/SSA DES possessed the minimum viscosity among these five DESs. DESs with low viscosity are accessible using small cations and/or fluorinated HBDs based on the hole theory, where vacancies with an average radius of about 2 Å are randomly distributed in the liquids.[46]

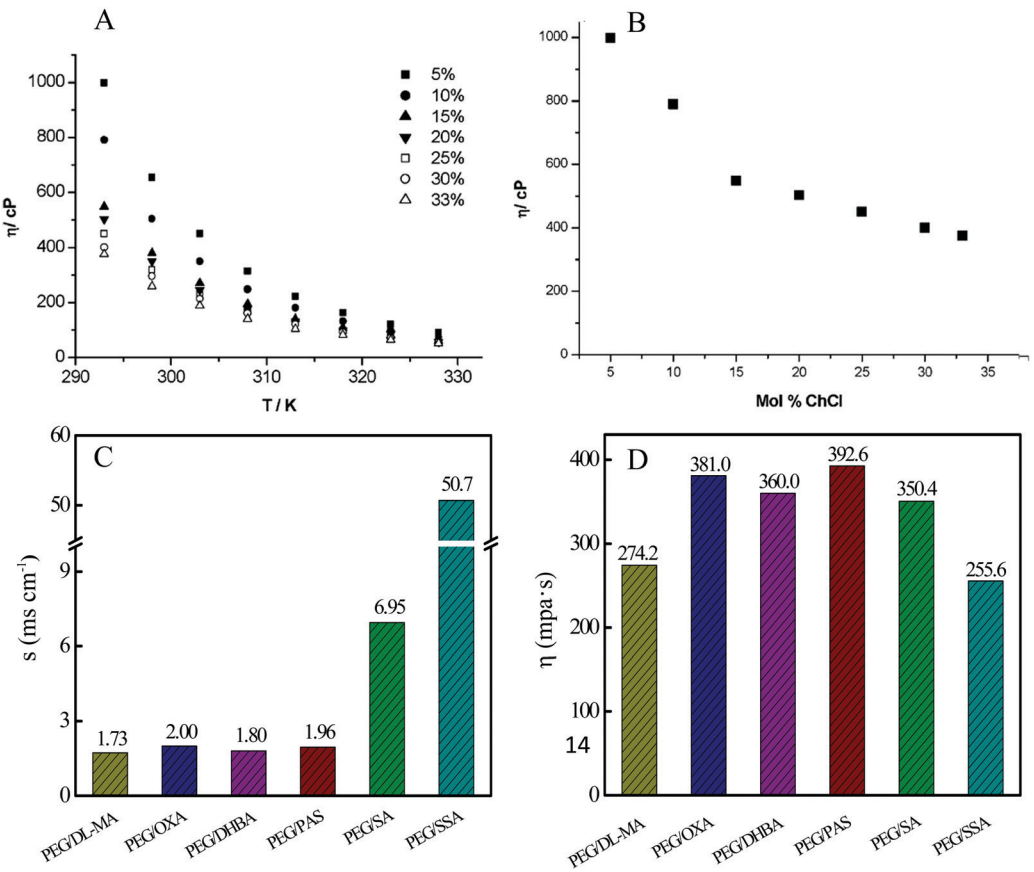

Fig. 5 Viscosity and conductivity of DESs. (A and B) The dependence of the viscosity of ChCl/glycerol DES on the temperature and ChCl composition. Reprinted with permission from ref. 52. (C) Conductivity and (D) viscosity of different DESs prepared from PEG and various organic acids measured at 60 °C. Reprinted with permission from ref. 47.

3.4. Ionic conductivity

The ionic conductivity is in direct proportion to the ionic migration rate within the DESs. Hence, this value is closely linked to the above-mentioned viscosity. The DES with low viscosity normally exhibited high conductivity such as PEG/SSA DES, as shown in Fig. 5. The molar ratio of HBD (benzenesulfonic acid, BSA) to HBA (PEG) significantly impacted the conductivity of BSA/PEG DES.[49] With the decrease of the PEG/BSA molar ratio, the conductivity of this DES system gradually increased. At PEG/BSA molar ratio = 1, it reached up to approximately 100 mS cm^{-1}.[49]

With the increase of the temperature, the conductivity of DESs increased due to the improved collision frequency of molecules. In addition, the conductivity can be determined by the following equations on the basis of the Walden rule.[53,54]

$$\Lambda \cdot \eta^{\alpha} = k$$

$$\log \Lambda = \log k + \alpha \log \eta^{-1}$$

Λ, η, and k are the mole conductivity, the dynamic viscosity, and a temperature-dependent constant, respectively. The dependence of $\log \Lambda$ on the $\log \eta^{-1}$ is defined as the Walden plot. In general, 1 mol L^{-1} aqueous KCl solution is taken as the reference, meaning the independent ions free of interactions for the dilute solution.[45,54,55] Cui *et al.* reported that the curves of ChCl/trichloroacetic acid, ChCl/monochloroacetic acid, and ChCl/propionic DESs below the ideal KCl solution line suggested that they were subionic, while ChCl/*p*-toluenesulfonic acid DES was not subionic (Fig. 6).[45]

3.5. Acidity

Acidity is considered to be a significant property for the practical applications of DESs, and particularly for catalytic applications.[56–58] Based on the acidic type, acidic DESs are divided into Lewis acidic DESs (LADESs) and Brønsted acidic DESs (BADESs). For LADESs, FT-IR of pyridine or ethanenitrile adsorption is a sensitive tool to determine the Lewis acidity. IR adsorption bands at around 1450 cm^{-1} for pyridine and in the range of 2250–2340 cm^{-1} for acetonitrile are characteristic Lewis acidity-related signals for LADESs.[51,59,60] Duan *et al.* utilized pyridine adsorption IR to test the Lewis acidity of $ChCl/ZnCl_2$ and benzyltrimethylammonium chloride (BTACl)/$ZnCl_2$ DESs. As shown in Fig. 7, the pure pyridine molecule exhibited a band at 1437 cm^{-1}, whereas the $ChCl/ZnCl_2$ and $BTACl/ZnCl_2$ DESs after pyridine adsorption displayed a 1448 cm^{-1} signal assigned to Lewis acidity. The absence of the 1540 cm^{-1} band could rule out the possibility of the existence of Brønsted acidity.[60]

Concerning BADESs, the Brønsted acidity is measured by the pH or Hammett function (H_0).[35,45,61] Kareem *et al.* investigated the influence of temperature on the pH of phosphonium-based DESs.[61] $Me(Ph)_3PBr$/glycerol DES possessed a neutral pH that was almost independent of temperature. However, the pH of $Me(Ph)_3PBr/CF_3CONH_2$ DES was as low as 2.5 at 25 °C, and was enhanced with the increase of temperature. Taysun *et al.* also measured the pH of three kinds of trimethylammonium chloride (BTMAC)-based DESs.[62] It was found that the pH value of DESs followed the sequence of BTMAC/*p*-toluenesulfonic acid > BTMAC/oxalic acid > BTMAC/citric acid (Fig. 7), which was closely related to the corresponding pK_a of HBDs (*i.e.*, organic acid). These results suggest that the temperature and the nature of the components significantly impacted the acidity of DESs.

The Hammett acidity function (H_0) obtained from UV-visible spectroscopy with a basic indicator (like 4-nitrobenzylcyanide) is also capable of assessing the acidity of DESs. This value is calculated by the following equation, $H_0 = pK[I] + \log([I^-]/[HI])$, where $pK[I]$, $[I^-]$, and [HI] indicate the ionization constant of the aqueous indicator, molar concentration of the anionic indicator, and molar concentration of the neutral indicator, respectively. A medium with low H_0 value manifests strong acidity.[63] Cui *et al.* employed H_0 to evaluate four ChCl-based DESs (ChCl/*p*-toluenesulfonic acid, ChCl/trichloroacetic acid, ChCl/monochloroacetic acid, and ChCl/propionic acid) (Fig. 6). ChCl/*p*-toluenesulfonic acid exhibited stronger acidity than the others, on account of the higher acidity of *p*-toluenesulfonic acid.[45] For the ChCl/urea system, the addition of a little water (1–3 wt%) enabled H_0 to decrease from 10.77 to 10.65 due to the partial solvation effect.[63] Wang *et al.* proposed that the acidity

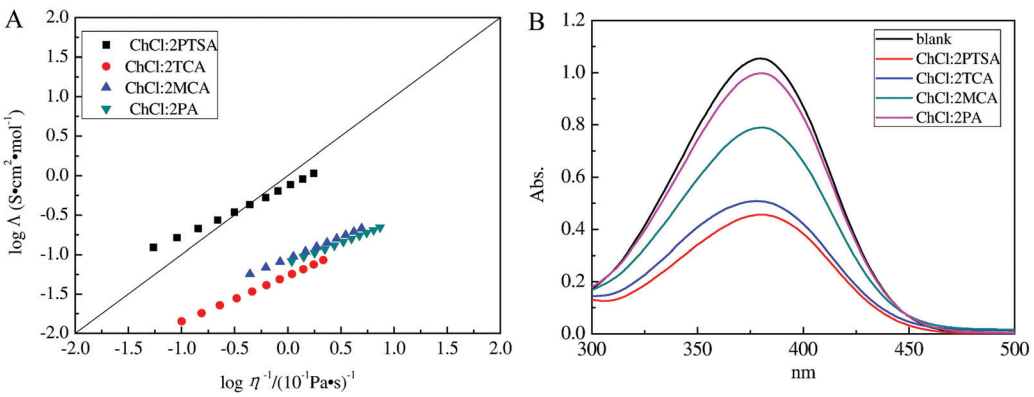

Fig. 6 (A) The dependence of $\log \Lambda$ on $\log \eta^{-1}$ for various DESs. The solid straight line is the ideal line for aqueous KCl solutions. (B) UV-vis absorbance spectra of 4-nitroaniline for different DESs in water. Reprinted with permission from ref. 45.

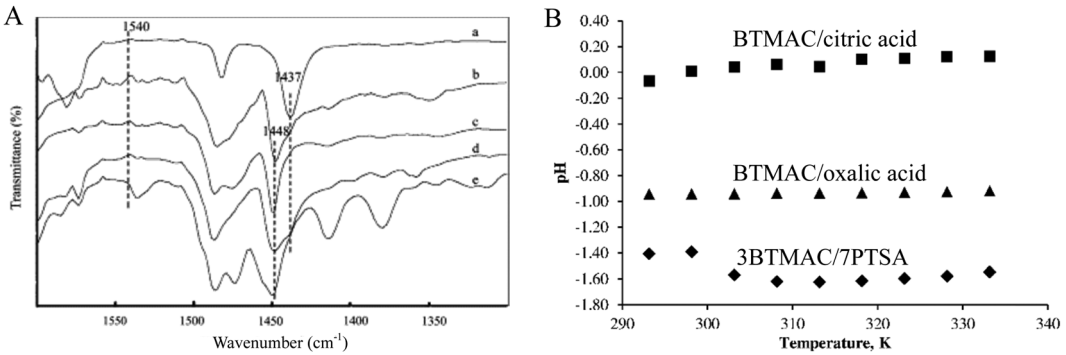

Fig. 7 (A) FT-IR spectra of (a) pure pyridine, (b) pyridine + choline chloride/$ZnCl_2$, (c) pyridine + choline chloride/$2ZnCl_2$, (d) pyridine + choline chloride/$3ZnCl_2$ and (e) pyridine + benzyltrimethylammonium chloride/$2ZnCl_2$. Reprinted with permission from ref. 60. (B) The dependence of pH on the temperature for three DESs. Reprinted with permission from ref. 62.

of the ternary DES (1-butyl-3-methylimidazolium chloride (BmimCl)/boric acid/glutaric acid, H_0 = 2.328) was stronger than that of binary DESs (BmimCl/BA, H_0 = 2.495; BmimCl/GA, H_0 = 2.481).[35]

3.6. Hydrophilicity/hydrophobicity

The majority of DESs reported in the literature are hydrophilic because they are prepared from common hydrophilic materials such as sugar, organic acid, and alcohol.[31,64] The main drawback of this hydrophilic DESs is instability when it is in contact with water. Thus, in 2015, two kinds of hydrophobic DESs (quaternary ammonium salts/decanoic acid, DL-menthol/carboxylic acids) were prepared by the Kroon and Marrucho groups.[65,66] So far, most of the hydrophobic DESs are composed of quaternary ammonium salt, alcohol, and acid with long alkyl chains. Florindo *et al.* prepared a series of hydrophobic DESs, which were made up of a fatty acid salt and another fatty acid.[67] Therefore, the choice of suitable HBAs and HBDs plays a key role in the formation of hydrophobic DESs. Commonly, the higher melting point depression for hydrophilic DESs compared to that for hydrophobic DESs is due to the strong hydrogen bond interactions derived from the existence of a charged and polar species.[31] Meanwhile, the thermal stability of the hydrophobic DESs is lower than that of the hydrophilic ones.

The water solubility of hydrophobic DESs is generally less than 7 wt%.[68–70] The presence of alkali metal ions and easily available charge on the central atom with one short alkyl chain contribute to a slightly increased water solubility.[31,67] For example, tetrabutylammonium chloride/decanoic acid and methyltrioctylammonium/decanoic acid DESs displayed relatively high water solubilities of 6.94 and 6.22 wt%, respectively.[67]

3.7. Polarity

The polarity scale, $E_T(30)$, is generally used to assess the polarity of a solvent, which is determined by the following equation in combination with UV-vis spectra and Reichardt's dye 30. $E_T(30)$ (kcal mol^{-1}) = $hc\nu_{max}N_A$ = (2.8591 × 10^{-3})ν_{max} (cm^{-1}) = 28 591/λ_{max} (nm), where ν_{max}, λ_{max}, h, c, and N_A are the maximum frequency, maximum wavelength, Planck constant, velocity of light, and Avogadro's constant, respectively.[25,52,71] Abbott *et al.* studied the polarity of ChCl/glycerol DES in terms of $E_T(30)$.[52] The similar polarity to ionic liquids with discrete anions for these series of DESs was observed.[52,72] Additionally, the value of $E_T(30)$ enhanced almost linearly with increasing molar content of ChCl. It should be noted that extrapolating this trend to 100% ChCl afforded an $E_T(30)$ value of about 59 kcal mol^{-1}, which is comparable to that of ethylammonium nitrate rather than ChCl.[52,72]

3.8. Surface tension

The values of the surface tension for DESs are usually larger than most conventional molecular solvents, which are similar to imidazolium-based ionic liquids (*e.g.*, 1-butyl-3-methylimidazolium tetrafluoroborate, 38.4 mN m^{-1} at 63 °C).[25,73] For instance, ChCl/ethylene glycol (EG) DES with a ChCl molar content of 15% and 30% showed 45.3 and 47.2 mN m^{-1}, respectively.[74] With respect to the ChCl/EG and ChCl/1,4-butanediol DESs, ChCl/glycerol DES exhibited higher surface tension derived from the three-dimensionally hydrogen bonded liquid of glycerol with three –OH species.[74] The surface tension follows a similar trend to viscosity since they are all indicators of intermolecular forces in the liquid. Consequently, a decreased trend for the surface tension was noticed with the increase of the ChCl molar ratio because the addition of ChCl broke up the formed structure between the –OH group and anion of ChCl.[52]

Hole theory is generally employed to explain the mobility of ions based on this expression, $4\pi r_H^2 = 3.5kT/\gamma$, in which r_H, k, T, and γ are average sizes of the void, Boltzmann constant, absolute temperature, and surface tension, respectively.[22,52] The comparable average size of the void contributes to the similar liquid properties between DESs and ionic liquids.[22] Moreover, for the ChCl/glycerol DES system, the surface tension was temperature-dependent and decreased linearly with the enhancement of the temperature, which is the same case with the phenomenon of ionic liquids.[52]

3.9. Diffusion

Gaining insight into the microscopic diffusion properties is of great significance for precisely constructing tailor-made DESs in

practical applications, and is beneficial for developing innovative DESs at the molecular level.[75–79] The pulsed field gradient nuclear magnetic resonance (PFG-NMR, generally employing ^{1}H NMR) technique is the most powerful approach for quantifying the molecular self-diffusion in liquid components.[77,80] This technique can encode and decode the translational diffusion motion of ions or molecules, depending on the magnetic field gradient pulses.[80] The diffusion coefficient D is determined by the equation, $E = \exp[-D\gamma_H{}^2 g^2 \delta^2 (\Delta - \delta/3)]$, where E, γ_H, g, δ, and Δ are the NMR signal attenuation, the gyromagnetic ratio of the nuclei, the strength of the gradient pulse, duration time, and observation time, respectively.[77,78]

It was found that increasing the temperature contributed to a weaker interaction between the choline cations and HBD for several choline chloride-based DESs (ethaline (choline chloride/ethylene glycol), glyceline (choline chloride/glycerol), reline (choline chloride/urea), and maline (choline chloride/malonic acid)).[77] The self-diffusivity was in the region of 10^{-10}–10^{-13} m^2 s^{-1}, meanwhile obeying the temperature-dependent Arrhenius equation, $D = D_0 \exp(-E_a/RT)$ (D_0, E_a, and R are a constant (m^2 S^{-1}), the activation energy (J mol^{-1}), the gas constant (J K^{-1} mol^{-1})).[77,79] The choline cation in ethaline, glyceline, and reline diffuses lower than the corresponding HBD, while the opposite trend was observed for maline, which was ascribed to the molecular size and molecular weight. The dramatic low self-diffusion coefficient values of the choline cations was due to the formation of considerable dimer chains for malonic acid.[77,81]

The diffusion property in the liquid mixture was tightly related to the ionic conductivity and viscosity.[79,82,83] The lower molar ionic conductivity of glycerol/NaOAc DES than that of glycerol/$Na_2B_4O_7{\cdot}10H_2O$ DES was due to the higher mobility of the glycerol hydroxyl protons in the latter one.[79] In general, the DESs with lower self-diffusion coefficients in terms of the ^{1}H species possessed higher viscosity.[52,79] Occasionally, the mobility of the sole ^{1}H-related species is not enough to understand the viscosity value. Compared to glycerol/NaBr DES, the larger mobility of the glycerol hydroxyl protons for glycerol/$Na_2B_4O_7{\cdot}10H_2O$ resulted in higher viscosity on account of the fact that $Na_2B_4O_7$ was positive to increase the viscosity.[79]

Considering these advantages, especially the low cost and simple preparation method with 100% atom utilization, DESs are appealing to green catalysis, organic synthesis, electrochemistry, dissolution process, extraction process, material science, and others.[84–87] In the following part, we compile interesting application examples of DESs in the desulfurization process of fuel oil, including extraction desulfurization, extraction–oxidation desulfurization, and the newly developed biomimetic extraction–oxidation desulfurization.

4. DESs-assisted extractive desulfurization

4.1. Influence of process factors

DESs with the remarkable feature of freezing point depression generally exist in the homogeneous state, whose physicochemical properties can be modulated by various types and molar ratios of HBAs and HBDs. When fuel oil and DESs are not mutually soluble, and the sulfide solubility in DESs is much higher than that in fuel oil, the extraction of sulfide from the fuel oil to DESs is possibly accomplished. In 2013, Li *et al.* synthesized a series of DESs with ChCl, tetramethyl ammonium chloride (TMAC), and tetrabutyl ammonium chloride (TBAC) as HBAs, and with malonic acid (MA), glycerol (Gl), tetraethylene glycerol (TEG), EG, PEG, and propionate (PR) as HBDs, which were first adopted in the desulfurization of model diesel as extraction agents.[88] This work opens the door for the application of DESs in the desulfurization process of fuel oil. Fueled by this pioneering research, the application of DESs in the extraction desulfurization (EDS) springs up,[89–94] which is summarized in Table 2. Normally,

Table 2 The performance of extraction desulfurization for DBT using various DESs[a]

No.	DES	HBA : HBD (mol : mol)	Mass ratio[b]	Temperature (°C)	Time (min)	Sulfur removal (%)	Ref.
1	ChCl/Pr	1 : 2	2 : 1	25	30	52.3	88
2	TBAC/Pr	1 : 2	2 : 1	25	30	82.0	88
3	TBAC/PEG	1 : 2	2 : 1	25	30	82.8	88
4	TBAC/PEG/$FeCl_3$	4 : 1	1 : 1	25	15	89.5	89
5	TEA/FO	1 : 2	N/A[c]	30	10	48.1	90
6	TEA/AC	1 : 3	N/A	30	10	49.4	90
7	TEA/PR	1 : 2	N/A	30	10	52.3	90
8	MIM/PA	N/A	2 : 1	30	N/A	84.6	91
9	DEA/PA	N/A	2 : 1	30	N/A	37.4	91
10	$SnCl_2$/TPPB	1 : 1	1 : 5	30	100	27.3	92
11	$SnCl_2$/TPPB	1 : 1	4 : 5	30	100	87.8	92
12	C_4DMEA/$FeCl_3$	1 : 1	1 : 5	50	10	39.0	93
13	C_{12}DMEA/$FeCl_3$	1 : 1	1 : 5	30	10	52.9	93
14	C_8DMEA/$FeCl_3$	1 : 1	1 : 5	30	10	51.5	93
15	BzDMEA/$FeCl_3$	1 : 1	1 : 5	30	10	39.2	93
16	BzMDEA/$FeCl_3$	1 : 1	1 : 5	30	10	37.6	93
17	TBAB/HCOOH	1 : 1	1 : 1	30	30	60.0	94
18	TBAB/OA	1 : 1	1 : 1	30	30	39.2	94

[a] Abbreviations: propanoic acid, PA; 1-methylimidazole, MIM; diethanolamine, DEA; $[CH_3(CH_2)_3]_4$PBr, TPPB; *N*,*N*-dimethylethanolamine, DMEA; *N*-methyldiethanolamine, MDEA; benzyl chloride, BzCl; oxalic acid, OA. [b] Indicating the mass ratio of DESs to fuel oil. [c] Indicating not available.

various sulfides, including thiophene, benzothiophene (BT), dibenzothiophene (DBT), and 4,6-dimethyldibenzothiophene (4,6-DMDBT), are mixed with the solvents, such as *n*-octane, *n*-heptane, and decahydronaphthalene, acting as the model fuel oil. Several parameters (the type of DESs, molar ratio of HBA to HBD, extraction time, extraction temperature, and the mass ratio of fuel oil to DESs) affect the desulfurization efficiency to some extent.

4.1.1. The type of DESs. Among these above-mentioned DESs in the literature,[88] under optimal conditions (DES/model oil mass ratio = 2 : 1, 25 °C, 30 min), the extraction efficiency of TBAC/PEG DES was 82.83% for one cycle. After five cycles, the extraction efficiency of up to 99.48% was achieved, corresponding to a sulfur content of below 8.5 ppm in the model diesel. In 2016, a ternary DES of TBAC/PEG/$FeCl_3$ exhibited a higher desulfurization efficiency of 89.53% in comparison to the previous binary TBAC/PEG DES.[89] Deep desulfurization of almost 100% was realized in only two cycles. It was found that the three components all influenced the extraction process following this sequence: for HBA, TBAC > tetraethylammonium chloride (TEAC) > ChCl; for HBD, PEG > propionic acid (PA) > GL > MA > benzoic acid (BA) > formic acid (FA); for metal ions, $FeCl_3$ > $ZnCl_2$ > $CuCl_2$ > $CoCl_2$ > $NiCl_2$. Wang *et al.* obtained three DESs by simply mixing triethylamine (TEA) with FA, acetic acid (AA), and PA, respectively, affording the sulfide removal ability of TEA/PA > TEA/AA > TEA/FA. This finding suggests that the long alkyl chain of an organic acid with high hydrophobicity is beneficial to the sulfide removal.[90]

The DESs type also influences the desulfurization efficiency of different refractory aromatic sulfides. Tang *et al.* constructed a series of DESs that are composed of $AlCl_3$, chlorinated paraffins, and aromatics for extraction desulfurization. The type of aromatics was closely related to the removal efficiency of sulfides, during which toluene exhibited better extraction performances than others (*p*-xylene, *o*-xylene, ethylbenzene, benzene, and chlorobenzene).[95] The removal efficiency of 3-methylthiophene, BT, and DBT reached 99.81%, 99.65%, and 89.64%, respectively. Gano *et al.* claimed that the extraction efficiencies of DBT and thiophene achieved 64% and 44%, respectively, using $FeCl_3$-based DESs.[92] In another study, tetrabutylammonium bromide (TBAB)/HCOOH DES possessed 81.75%, 80.47%, and 72.00% extraction efficiencies of BT, DBT, and thiophene in model oil, respectively.[94] This experiment phenomenon was explained in terms of the electron density and steric hindrance for different sulfides. Zhao *et al.* reported that triethylamine/benzoic acid showed 58.06%, 70.61%, and 78.30% removal efficiencies for thiophene, BT, and DBT, respectively.[96] From these results, a conclusion can be made that different DESs exhibit disparate selectivity in sulfide removal. For a specific sulfide removal, not only electron density and steric hindrance, but also the component of DESs should be taken into consideration.

4.1.2. Molar ratio of HBA to HBD. Wang *et al.* found that the molar ratio of the base (HBA) to acid (HBD) greatly affected the DESs solubility in fuel oil and the desulfurization ability.[90] When the HBD/HBA = 3 or 5, the DES solubility reached the minimum at below 0.003%. Increasing the propionic acid/triethylamine molar ratio in DES from 2 to 5 led to the decreased extractive desulfurization, which was likely on account of the depression of hydrogen bond interactions resulting from the steric hindrance of the increased carbon chains.[97] For the ternary DES of TBAC/PEG/$FeCl_3$, the optimal molar ratio was 4 : 1 : 0.05 for sulfide elimination, corresponding to a desulfurization efficiency of approximate 89.53%. The reason of the influence of the molar component on desulfurization may be the different sulfide solubilities in DESs.[89]

4.1.3. Extraction time and temperature. For ChCl/PR, TBAC/PR, and TBAC/PEG DESs, the extraction equilibrium was achieved within as short as 10 min, accompanied by an extraction efficiency of about 71%. It was speculated that the fast equilibrium came from the relatively low viscosity and high extraction capability of the corresponding DESs.[88] In addition, a higher temperature was not advantageous for this extraction process. Satisfactorily, this technology can be performed at 25 °C under ambient pressure with sulfur removal of about 70%, which was valuable for industrial applications.[88] In 2016, Li *et al.* reported a shorter equilibrium time of 5 min for a new ternary DES with an extraction efficiency of about 90%.[89] With respect to other DESs, similar results were observed.[90,93] Regarding the extraction temperature, a low temperature was favorable because the extraction process was exothermic. In addition, decreasing the temperature resulted in increasing the viscosity of DESs and partitioning coefficient (K_N). Thus, there is a trade off between the thermodynamics and kinetics process. Wang *et al.* proposed that the K_N value was enough for trimethylamine/organic acid DESs.[90] From these studies in the literature, we know that extraction desulfurization is usually performed at room temperature with ambient pressure, which is the point of this technology being attractive for practical applications in view of energy consumption, security, and desulfurization efficiency.

4.1.4. Mass ratio of fuel oil to DESs. With the increasing mass ratio of TBAC/PEG DES to model oil, the extraction efficiency was sharply enhanced at the beginning, and then increased slowly. Considering the expense and extraction performance, the mass ratio of DES to fuel was chosen as 1.[88] Lu *et al.* prepared the piperazinium-based ionic liquids with a lactate anion, which in fact, should be called DESs.[98] For each sulfide, the analogical trend was observed as the above study. Additionally, at the mass ratio of DES/fuel below 1, BT was more sensitive to the change of the DES amounts in comparison with TS, DBT, and 4,6-DMDBT, while these four sulfides exhibited almost similar sensitivity at high DES/fuel mass ratio.[94] Numerous studies in the literature reported similar results.[93,99] The fuel oil and DESs are immiscible, forming two phase systems. Depending on Fick's law, the DESs dosage greatly affected the mass transfer of sulfide from the fuel oil phase to the DESs phase. Normally, it is expected that employing a lower dosage of DESs gives rise to better extraction desulfurization at an industrial scale.

4.2. Extraction mechanism

Unveiling the extraction mechanism is significant for establishing the structure–performance relationship during the extraction

process on a molecular level, which will provide guidance for designing task-specific DESs as an extraction agent. Li *et al.* used ^{1}H NMR and FT-IR spectroscopy to investigate this issue (Fig. 8A and B).[88] The hydrogen bond interaction between the active hydrogen of DES and the sulfur atom in BT strengthens the electron-withdrawing ability of the sulfur atom to the hydrogen atoms in BT, resulting in the decrease of electron density for the molecular ring. Therefore, the hydrogen bond between the sulfide and DESs was the main driving force for this extraction desulfurization, which was similar to that of the ternary metal ions-based DESs.[89]

For arenium ion-based DESs, the migration of the sulfide from the fuel oil to the DESs phase occurred *via* formation of liquid clathrate and a complex, which mainly depended on the π–π interaction and complexation between the aromatic sulfide and DES.[95] Unfortunately, a trace of aromatic was moved from the DESs phase to oil phase (Fig. 8C). ^{1}H NMR analysis and density functional theory (DFT) were employed to detect the extraction mechanism of the triethylamine/propionic acid DES. Li *et al.* pointed out that both hydrogen bond interaction and CH–π interaction were responsible for the excellent extraction desulfurization (Fig. 8D).[90]

The nature of the interactions between the organic sulfides and DESs was analyzed by experimental and theoretical studies. The electrostatic potential (ESP) and reduced density gradient (RDG) analyses revealed that the outstanding extraction performance of the aromatic acid-based DESs predominantly came from van der Waals and other non-covalent interactions, as shown in Fig. 8E.[96]

In short summary, the strong interaction between the DESs and sulfur compounds existing in the form of the hydrogen bond, CH–π interaction, van der Waals, and other non-covalent interactions contributes to this unique behavior of DESs for extraction desulfurization.

5. DESs-assisted extraction–oxidation desulfurization

To realize ultra-deep desulfurization in one single stage, one strategy is the combination of extraction technology with oxidation desulfurization, namely extraction and catalytic oxidation desulfurization (ECODS). At the early stage, DESs are just deemed as only substitutions of organic solvents and traditional ionic liquids.[21,100] Recently, functionalization has become one of the promising development directions for DESs.[28] Selecting some compounds with specific functional groups as HBAs or HBDs can precisely tailor the physicochemical properties of DESs.[31] Then, some characteristics like catalytic oxidation will come into being. Functionalized DESs were demonstrated to play multifunctional roles in extraction agents, reaction media, and catalysts during the process of ECODS.[39,101]

The typical process of ECODS is presented as follows. DESs and fuel oil are immiscible. Two phases exist in the ECODS systems, during which fuel oil is located above. The sulfur compounds extract from the upper oil phase to below the DESs phase. The catalytically oxidative products of sulfones are dissolved in the DESs phase. Clean fuel oil is obtained by means of the decanting method. When the DESs are hydrophilic, introducing appropriate water into DESs can make sulfones existing in the solid state separate out. These oxidation products of sulfones can be filtered out and the residual water in DESs is removed by reduced pressure distillation, achieving the regeneration of DESs.[102] As mentioned above, we know that the oxidant is an indispensable factor for this process. Considering the cost, safety, availability, and environmental friendliness, hydrogen peroxide (H_2O_2), molecule oxygen (O_2), organic peracid, and organic hydroperoxide are usually selected as oxidants.[101–104]

5.1. Employing H_2O_2 as an oxidant

H_2O_2 is intensively utilized as a green oxidant because the sole byproduct is water. In 2015, the Lü group synthesized a series of DESs with the HBAs of ChCl, TMAC, and TBAC, respectively, and with the HBDs of oxalic acid (OA) for the application of ECODS.[105] When the volume ratio of fuel oil to TBAC/OA DES was as high as 5, it still exhibited excellent desulfurization efficiencies up to 98%. It was also found that the type and molar ratio of HBA and HBD were tightly associated with the catalytic performances. The desulfurization mechanism followed the dual activation model. The weakness of the aromaticity in DBT derived from the strong interaction between the DESs and DBT made it susceptible to being oxidized. Meanwhile, the carboxylic acids in DESs were oxidized to peracids by H_2O_2, which served as an oxidant to catalyze the DBT transformation. At the same time, the peracids were converted to carboxylic acid to restart another catalytic cycle.[105] The acetamide/*p*-toluenesulfonic acid (*p*-TsOH) DES showed the outstanding desulfurization performance of DBT in the model diesel (100%) and actual commercial diesel (98%). The dual activation mechanism was also appropriate for this DES system.[106]

In the same year, Li *et al.* used ChCl/*p*-TsOH DESs to proceed ECODS for model oil and real oil.[104] Under optimized conditions, the S-compound removal reached 99.99% with the DES/fuel mass ratio of 0.5. The authors also proposed that the desulfurization efficiency was positively correlated with the acidity of the corresponding DESs, which was different from the extraction desulfurization process reported by Tang *et al.*[95] The functional group of the alcoholic hydroxyl group in ChCl was of paramount importance for the production of the active oxygen species in ChCl/*p*-TsOH DES. Notably, the ECODS process also obeyed the extraction–oxidation mechanism (Fig. 9).[104] Mao *et al.* reported that the desulfurization efficiency reached 68.5% for the real diesel oil with the assistance of ChCl/CF_3SO_3H DES, using H_2O_2 as an oxidant.[107]

In 2017, Hao *et al.* introduced L-proline-based DESs in attempt to establish the relationship between the acidity of DESs and desulfurization capability.[102] However, it was revealed that there was no direct correlation for these two factors. Meanwhile, the good stability of L-proline/*p*-TsOH DES was further confirmed using electrochemical measurement and recycle experiment (Fig. 9).[102]

Although the hydrogen bond interaction plays a significant role in the dual activation for ECODS systems, the component–structure–performance relationship for the DESs component,

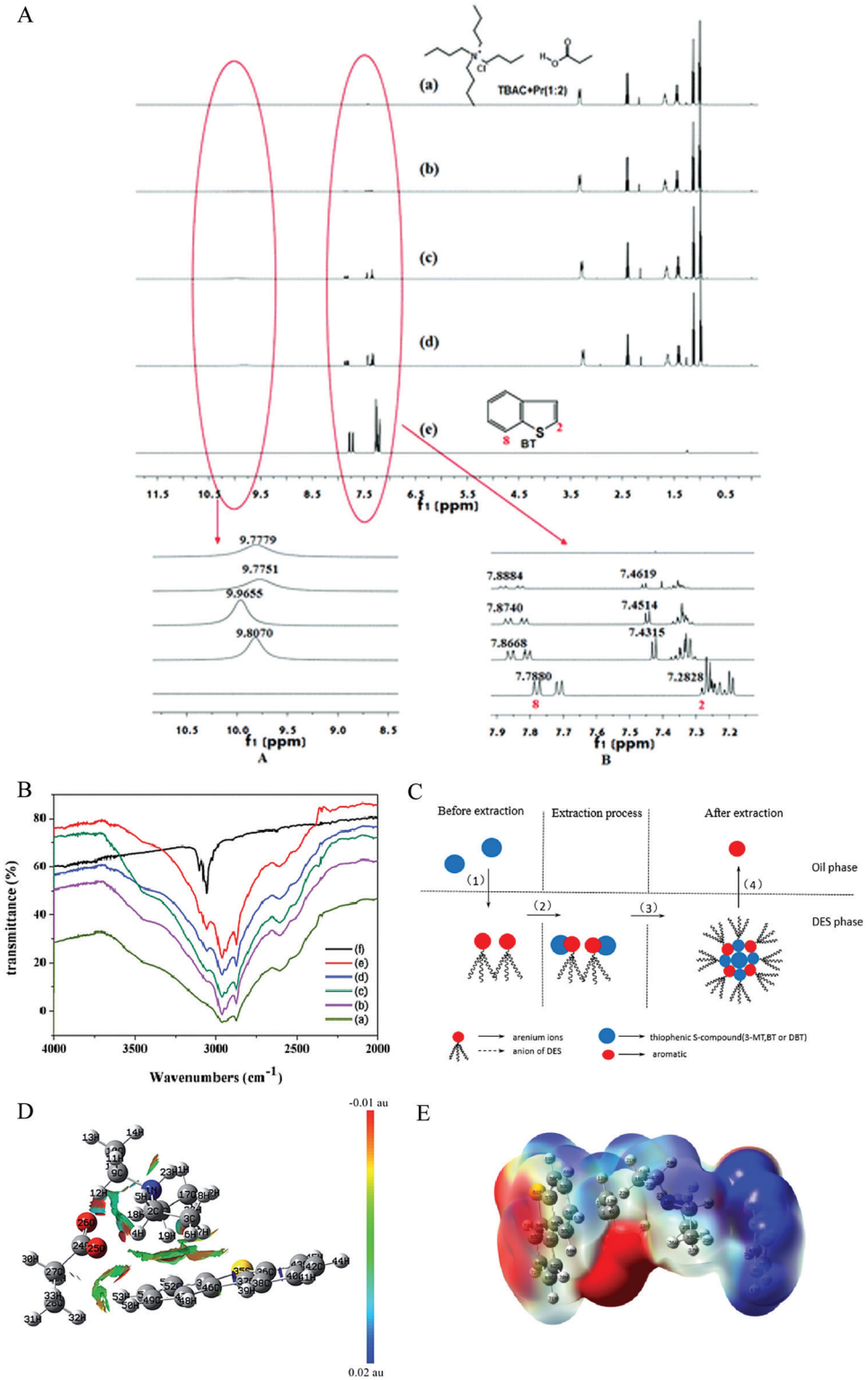

Fig. 8 (A) ^{1}H NMR of different molar ratios (TBAC + Pr/BT). (a) 1 : 0, (b) 1 : 0.1, (c) 1 : 0.5, (d) 1 : 1, (e) 0 : 1. Reproduced from ref. 88 with permission from the Royal Society of C hemistry. (B) FT-IR spectra of different molar ratios (TBAC + Pr/BT). (a) 1 : 0, (b) 1 : 0.5, (c) 1 : 1, (d) 1 : 1.5, (e) 1 : 4, (f) 0 : 1. Reproduced from ref. 88 with permission from the Royal Society of Chemistry. (C) Process of extractive desulfurization. The DESs were prepared by using $AlCl_3$, chlorinated paraffins, and various aromatics. Reprinted with permission from ref. 95. Copyright (2015) American Chemical Society. (D) Gradient isosurfaces of triethylammonium propionate DES and DBT for the most stable configuration during extractive desulfurization. Red indicates strong attractive interactions, and blue indicates a strong nonbonded overlap. Reproduced from ref. 90 with permission from the Royal Society of Chemistry. (E) ESPs mapped on the electron total density with an isovalue of 0.001 a.u. The colors range from −12.6 kcal mol^{-1} (−0.0200 a.u.) in red, 0 kcal mol^{-1} in white, and +12.6 kcal mol^{-1} (+0.0200 a.u.) in blue for [TEA]/[BA]···DBT. Reprinted with permission from ref. 96.

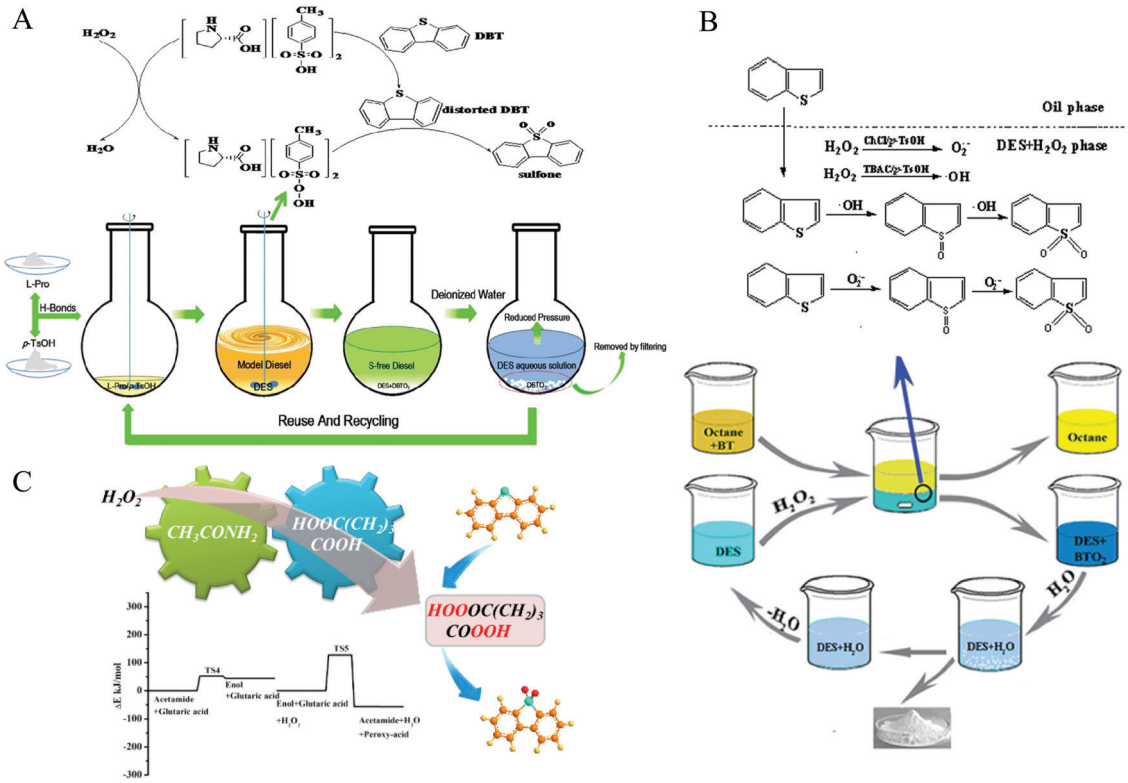

Fig. 9 The mechanism of extraction–oxidation desulfurization using DESs with H_2O_2 as an oxidant. (A) L-Proline/*p*-TsOH DES system. Reprinted with permission from ref. 102. (B) ChCl/*p*-TsOH DES system. Reproduced from ref. 104 with permission from the Royal Society of Chemistry. (C) The reaction potential energy of the oxidation of glutaric acid with the assistance of acetamide. Reprinted with permission from ref. 39.

hydrogen bond strength, and desulfurization performance is not well-established due to the presence of the hydrogen bond puzzle.[108] The investigation of caprolactam-based DESs confirmed that the hydrogen bond strength was in close connection with the sulfur removal. The higher hydrogen bond strength was helpful for the boost of the S-compound removal, which could be regulated by assembling different HBAs and HBDs together.[109]

DFT is a robust tool to study the reaction mechanism of the oxidative desulfurization on the molecular level.[39] In the case of the acetamide/glutaric acid DESs (Fig. 9), the higher transition state (TS) barrier of glutaric acid oxidation (in comparison with DBT oxidation) indicated that the former was the rate-limited process. The presence of acetamide significantly decreased the TS potential from 273.4 to 127.2 kJ mol^{-1} mainly through decreasing the glutaric acid oxidation by H_2O_2. The cooperation of acetamide and carboxylate-like enzyme catalysis is the origin of the excellent catalytic performance for DBT oxidation in DESs media.[39]

5.2. Employing O_2 as an oxidant through a biomimetic route

Although DESs can achieve the deep oxidation desulfurization of fuel oil using H_2O_2 as an oxidant, some fatal drawbacks that are still stumbling blocks for industrialized applications are as follows: (1) H_2O_2 is relatively expensive; (2) it is capable of bringing about dangers, such as explosion and deflagration, in the process of the transportation and storage for aqueous H_2O_2, particularly at high concentration.[110–112]

The application of molecular O_2 as an oxidant for oxidative desulfurization has received great interest due to its low cost, ease of availability, and environmental friendliness.[113] However, the oxidation of S-compounds in fuel oil is extremely difficult owing to the high activation energy barrier of O_2 with a triplet ground state.[112] Consequently, the oxidation is usually performed at high temperature and/or in the presence of sacrificial agents.[114–118] Non-selective free radical reactions easily take place at high temperature (generally above 100 °C), giving rise to the loss and reduction in quality for fuel oil. In addition, the utilization of sacrificial agents makes the operation and separation expense enhance sharply. Murata *et al.* achieved the oxidation desulfurization using Co-based salts as catalysts with the assistance of caprylaldehyde.[116] The sacrificial agent of caprylaldehyde was first oxidized to the corresponding peracid, which then catalytically oxidized the sulfides in fuel oil. As a result, the cost of this desulfurization technology would be expensive. Sampanthar *et al.* performed this process over metal oxide supported γ-Al_2O_3 with O_2 as the oxidant.[117] The high temperature of 130–180 °C gave rise to oxidation of the aromatic hydrocarbon, besides sulfur compounds, bringing about the loss of fuel oil. Li *et al.* took advantage of an amphiphilic polyoxometalate catalyst in emulsion droplets to carry out the aerobic oxidation desulfurization with isobutyraldehyde.[118] Therefore, the key issue of aerobic oxidative desulfurization (AODS) is O_2 activation under mild reaction conditions without the need for the help of any sacrificial agents.

In nature, biologically aerobic oxidation is generally processed under extremely mild conditions even at room temperature with ambient pressure. Numerous elemental reactions with coupled relationships are involved in the whole process, thereby circumventing the unfavorable kinetics of direct aerobic oxidation.[112] In the respiratory chain, there are several enzyme complexes serving as a redox trigger (Fig. 10). Oxygen obtains electrons from an electron-rich donor *via* multistep redox

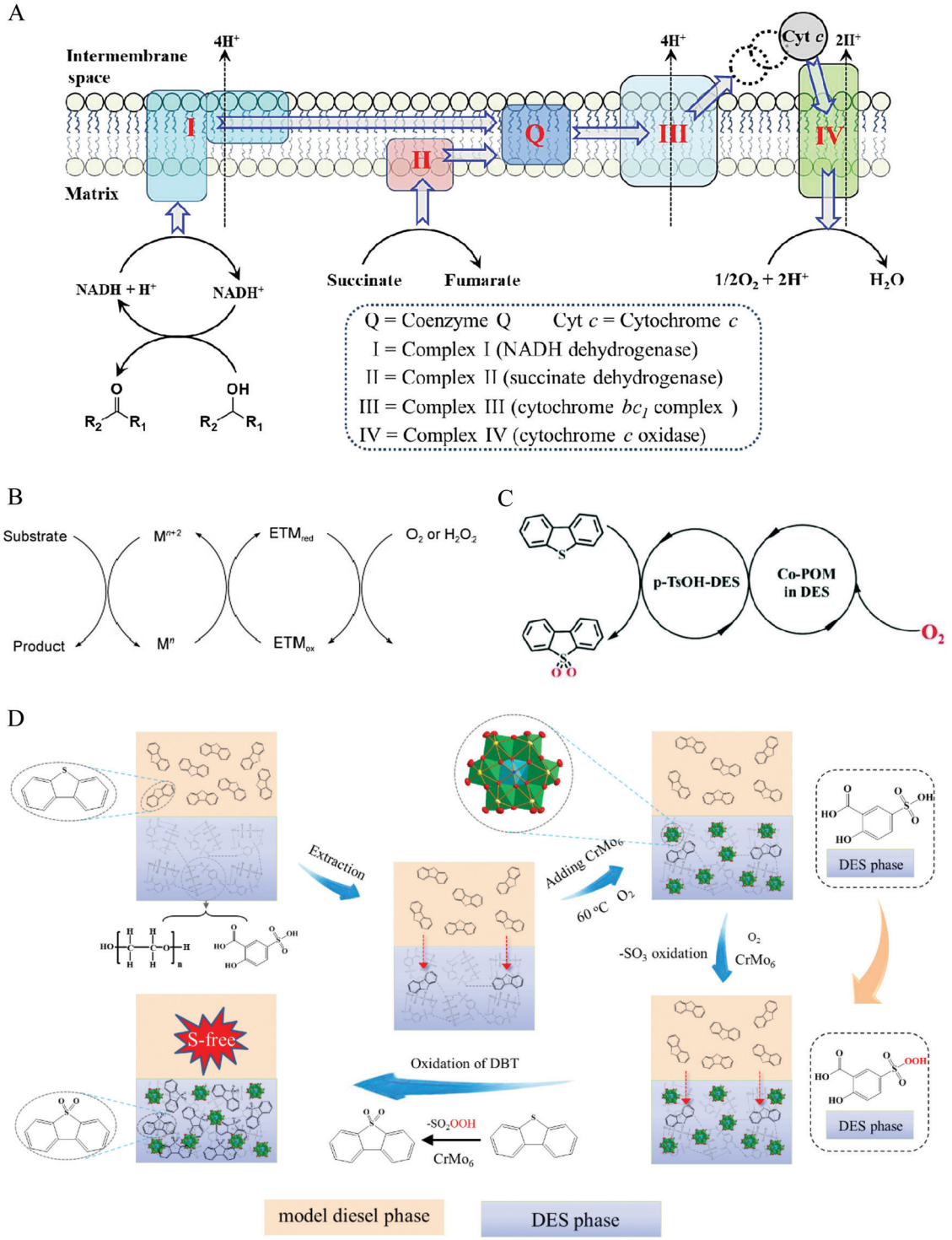

Fig. 10 Aerobic extraction–oxidation desulfurization *via* a biomimetic route. (A) Aerobic respiratory chain (electron transfer). (B) Electron transfer facilitated by an electron-transfer mediator (ETM). Fig. 10A and B are reprinted with permission from ref. 112. (C) A possible electron transfer of the biomimetic AODS process. Reproduced from ref. 113 with permission from the Royal Society of Chemistry. (D) The proposed mechanism for the EAODS process of coupling polyoxometalate with DESs. Reprinted with permission from ref. 47.

processes. For instance, the electron passes from NADH as an electron-rich donor to the terminal oxidant of O_2 through NADH dehydrogenase, coenzyme Q, cytochrome bc_1 complex, cytochrome *c*, and cytochrome *c* oxidase, to realize O_2 activation. Subsequently, the formed NAD^+ oxidizes alcohol to the product of aldehyde. These intermediate species, such as coenzyme Q and cytochrome *c* acting as the role of bridge for electron transmission, are referred to as electron transfer mediators (ETMs).[119,120]

The sulfides in fuel cannot be oxidized by O_2 in DESs media under mild conditions, for example, at the temperature of below 80 °C and ambient pressure.[47] Inspired by biologically aerobic oxidation systems, introducing an ETM between DESs and O_2 may be a strategy to accomplish aerobic oxidation desulfurization, avoiding the high activation energy of O_2 for the direct redox route.

Polyoxometalates (POMs) composed of metal oxide clusters exhibit the advantages of component diversity, thermodynamic stability, abundant topologies, tunability of redox and acid.[121–123] They are intensively applied in oxidative desulfurization. In 2010, Lü *et al.* reported amphiphilic Anderson catalysts for AODS.[124] The quaternary ammonium cations tremendously affected the catalytic activities, and $[(C_{18}H_{37})_2N(CH_3)_2]_5IMo_6O_{24}$ could completely oxidize sulfides without any sacrificial agents. Subsequently, a B-type Anderson $[(C_{18}H_{37})_2N(CH_3)_2]_3Co(OH)_6Mo_6O_{18}$ catalyst was used to perform AODS, demonstrating the distinctive catalytic activities in terms of the turnover number (4200) for DBT oxidation at 80 °C under ambient pressure.[125] Recently, a vanadium-substituted polyoxometalate modified by ILs exhibited 98.9% of DBT removal under optimal conditions (120 °C and 5 h).[126] However, these POMs are homogeneously dissolved in the fuel oil phase, causing difficulty in the catalyst reusability and recoverability.

From the abovementioned literature, it is known that O_2 can be activated by POMs under relatively mild conditions. The central metal–oxygen octahedron in the Anderson-type POMs is surrounded by six edge-sharing MO_6 (M = metal) octahedrons, displaying an attractive planar structure. Moreover, each circumambient framework metal atom has two terminal O atoms, which are generally considered as the active sites during the oxidation processes.[113,127] Therefore, it is inferred that POMs are ideal ETMs to lower the reaction activation energy of AODS in DESs media under more mild conditions.

If DESs are coupled with POMs in the AODS, sulfur compounds are extracted from the fuel oil phase to DESs phase. The whole process is called extraction and aerobic oxidation desulfurization (EAODS). In 2019, the Lü group first proposed a biomimetic approach depending on the combination of *p*-TsOH based DESs and $(NH_4)_3Co(OH)_6Mo_6O_{18}$ (Co-POM) for EAODS, where *p*-TsOH in DESs and Co-POM dissolved in DESs served as the electron donors and ETM, respectively.[113] The DBT removal reached 99% at 60 °C in 1 h without any sacrificial agents. The UV-vis spectra indicated that the presence of ETMs facilitated the electron transfer from Co-POM to the oxidant (O_2) along a pathway with low energy (Fig. 10).[113]

With the purpose of deeply understanding this biomimetic EAODS, a series of organic acids (such as DHBA, SSA, SA, OXA, PAS, and DL-MA) were chosen as the HBD.[47] PEG2000 and $Na_3H_6CrMo_6O_{24}$ (Cr-POM) were utilized as the HBA and ETM, respectively. Among these DESs, PEG/SSA with high conductivity and low viscosity displayed the best desulfurization efficiencies, corresponding to 100% at 60 °C within 2 h. The fuel oil and DESs were immiscible. The upper oil phase of the fuel oil was collected *via* decantation. The lower DES phase consisting of DES, Cr-POM, and products, was recovered using a rotary evaporator to remove a little water from the catalytic reactions. It should be noted that this system could be recycled four times without any obvious decrease of the catalytic activities for DBT, overcoming the disadvantages of sole POMs as catalysts. In combination with UV-vis, FT-IR, and experimental results, a reaction mechanism was proposed in which peroxypolyoxoanion was generated from Cr-POM with the assistance of O_2 and PEG/SSA DES, which successively oxidized the $-SO_3H$ group in SSA to peroxysulfonic acid. Electron-rich S atoms in DBT were then oxidized by this peroxyacid. Meanwhile, peroxyacid was reduced to $-SO_3H$ (Fig. 10), accomplishing one catalytic cycle.[47]

Very recently, the biomimetic EAODS system coupling Fe-Anderson type polyoxometalates (Fe-POMs) with benzenesulfonic acid (BSA)-based deep eutectic solvents (DESs) were constructed to unravel the influence of the DESs component.[49] It was found that the component of PEG/BSA DES intensively affected the catalytic performances of DBT oxidation. PEG/BSA DES with the molar ratio of 1 : 2.5 exhibited the best catalytic activities, which probably resulted from the higher hydrogen bond strength. This catalytic system was also effective for commercially available diesel, affording a desulfurization efficiency of 94% at 60 °C.[49] Whereafter, the current density determined from cyclic voltammogram characterization was 17-fold higher in comparison to that for the case without adding POMs. In combination with UV-vis analyses, it was confirmed that oxygen was activated, giving the decrease of the aerobic oxidation reaction barrier (Fig. 11).[128]

Therefore, this biomimetic approach overcomes the difficulty of O_2 activation by coupling DESs with polyoxometallates (POMs), in which DESs act as catalysts and POMs serve as ETM. This strategy is inspirational since biomimetic or bioinspired catalysis is the ''Holy Grail'' of oxidation catalysis. Owing to their advantages, such as strong ability to activate dioxygen, high reaction efficiency and mild reaction conditions, the DESs biomimetic approach provides a novel way not only for EAODS, but also for catalysis oxidation, such as the selective oxyfunctionalization of hydrocarbon.

Besides H_2O_2 and O_2, peroxymonosulfate (PMS) is also employed in the DESs-assistant oxidation desulfurization.[129] PMS, a white solid powder, is popular in the field of waste water treatment.[130] The solid phase below 65 °C makes it possible to store and transport. Using the PMS as an oxidant, $CoCl_2$–ChCl/PEG DES showed nearly 100% DBT removal at the extremely low temperature of 20 °C within 60 min.[129] It is speculated that the byproduct of sulfate will be generated from the reduced PMS, remaining in the fuel oil and/or DESs phase as contamination.

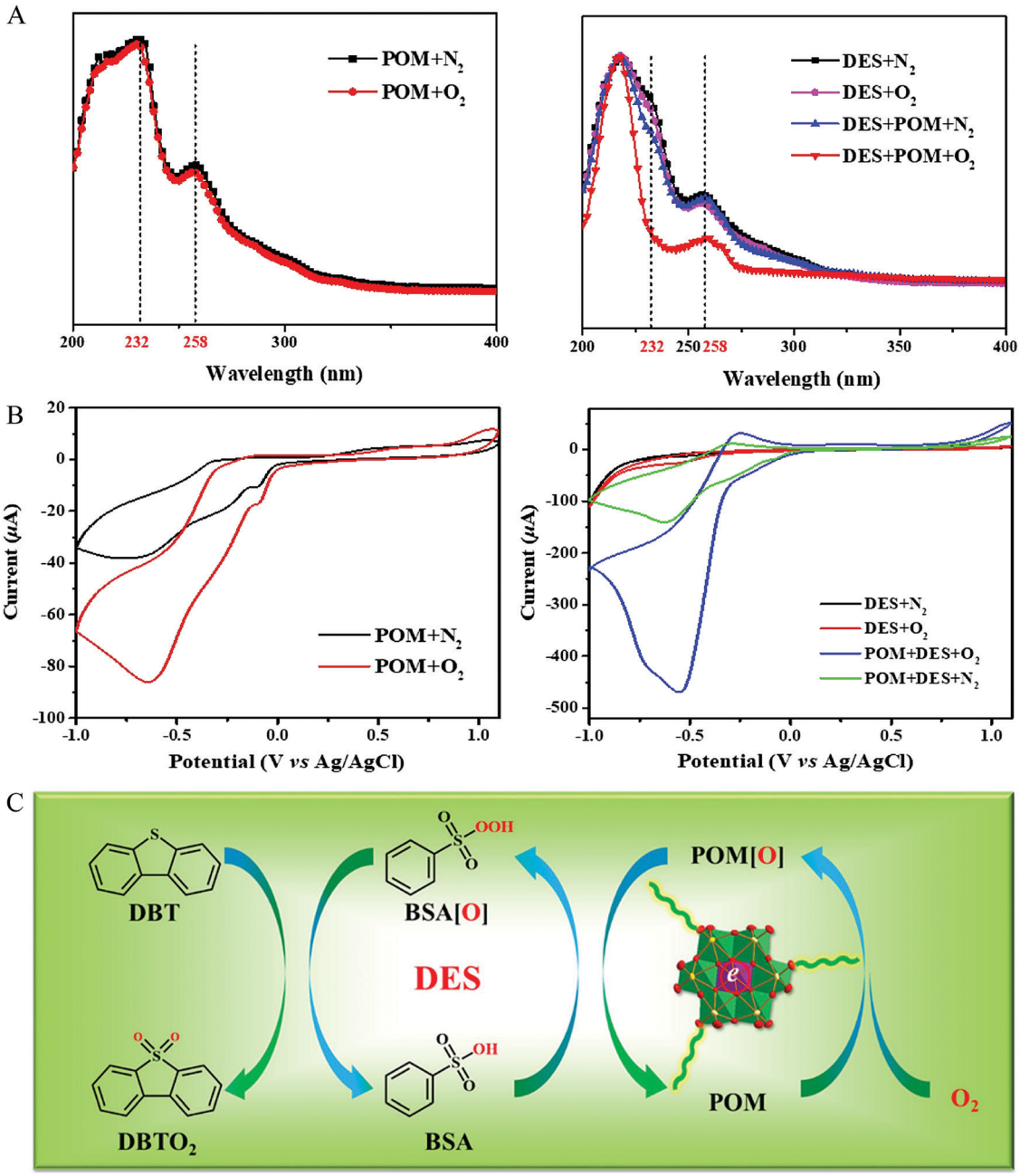

Fig. 11 (A) UV-vis spectrum, (B) cyclic voltammograms curves, and (C) proposed dual activated catalytic cycle for the biomimetic oxidative desulfurization. The DES and POM indicated the PEG/BSA and Fe-Anderson type polyoxometalates, respectively. Reprinted with permission from ref. 128.

6. Conclusions and perspectives

Driven by the great demands of green solvents in the scientific and industrial manufacturing communities, the studies for the synthesis, properties, and applications of DESs have rapidly multiplied since 2003. This review summarizes the physicochemical properties (freezing point, density, viscosity, ionic conductivity, acidity, hydrophilicity/hydrophobicity, polarity, surface tension, and diffusion) of DESs, and its application in desulfurization process for fuel oil. These properties can be tailored almost infinitely by adjusting the nature and molar ratio of HBAs and HBDs, affording the chances to prepare task-specific DESs. More interestingly, some properties are coupled with each other, rather than independent parameters. For example, the ionic conductivity is inversely related to the viscosity. Additionally, it should be noted that the thermal stability of some components of quaternary ammonium (like ChCl) is not conducive because the elevated temperature might trigger a Hoffman elimination reaction for ChCl. Compared to conventional ILs, DESs exhibited unique features, as follows: (i) 100% atom utilization in the synthesis process; (ii) low cost due to the easy accessibility of raw materials (even some are nature chemicals); (iii) low toxicity; (iv) negligible vapor pressure; (v) renewability and biodegradability. These features enable DESs

to be adopted in many fields, such as catalysis, organic synthesis, electrochemistry, analytical chemistry, chromatography, dissolution process, extraction technology, and material science. In particular, the effectiveness of DESs in degrading the recalcitrant structure in biomass facilitates their applications in transforming the biomass into biofuels and value-added chemicals.

DESs are ideal solvents for the extraction desulfurization. Numerous factors comprising the DESs type, molar ratio of HBA to HBD, extraction time, extraction temperature, and the mass ratio of fuel oil to DESs are closely related to the desulfurization efficiency. It should be noted that a low temperature is favorable for the improvement of sulfur removal, which is very attractive for future industrial applications. Increasing the temperature will make the viscosity decrease, facilitating mass transfer. Nonetheless, the extraction process is exothermic, meaning that increasing temperature will reduce the partitioning coefficient. On the whole, thermodynamics dominates this extraction process. Moreover, the strong interactions between DESs and sulfur compounds in the form of the hydrogen bond, CH–π interaction, van der Waals, and other non-covalent interactions are the main driving forces. Hence, further screening of the aromatic-derived compounds for the tailor-made design of DESs is essential. At present, desulfurization efficiency in one single stage is still relatively low. The relationship of the phase equilibrium needs to be addressed in the future because this parameter is the basis for designing and optimizing equipment, as well as evaluating the feasibility of the extraction technology. Eventually, the solubility of DESs in fuel oil remarkably influences the extraction desulfurization process, which is urgently desired for systematic investigation.

The integration of extraction with oxidation desulfurization is an effective method to achieve ultra-deep desulfurization in one single stage. The following features, challenges, and future directions accompany this process:

(1) DESs composed of HBAs and HBDs with specific functional groups, like the sulfonic acid group, possess unique catalytic performance. Task-specific DESs can be precisely designed by selecting suitable HBAs and/or HBDs. Meanwhile, DESs play multifunctional roles of extraction agents, reaction solvent, and catalysts during the process of ECODS. When they are hydrophilic, DESs are capable of recycling and regenerating *via* washing with water.

(2) H_2O_2 is generally used as an oxidant because the sole byproduct is water. Considering the security and cost of aqueous H_2O_2, O_2 is an ideal candidate for AODS due to its low cost, easy availability, and environmental friendliness. This AODS process is usually performed at high temperature and/or in the presence of sacrificial agents due to the high activation energy barrier of O_2. In order to settle these problems, a biomimetic approach is proposed to achieve EAODS under mild conditions (60 °C and ambient pressure). POMs are employed as ETMs, which works well in EAODS coupling with DESs. The electrons are transferred from the initial organic sulfides to the final molecular O_2, intermediately going through DESs and POMs in successive steps just like a relay athlete, which cannot be achieved by exclusively ILs, DESs or POMs.

(3) In the reported catalytic systems, POMs are dissolved in DESs, resulting in their difficulty in recovery. Encapsulation of POMs within porous solid matrixes, such as zeolites and metal organic framework for constructing composite materials, may be a potential solution.

(4) Exploration on the modification of DESs and POMs *via* various alkyl chains and/or ions might be alternative approaches to further enhance the desulfurization performances from the perspective of the hydrophilicity/hydrophobicity and microenvironment for active sites.

(5) *In situ* technologies, such as Raman and ambient-pressure XPS, should be undertaken to understand the transformation of the active sites, deeply shedding light on the catalytic mechanism.

(6) It is necessary to seek other ETMs, like metal oxide, for the substitution of POMs to further boost the catalytic performances.

(7) Molecular dynamic simulation (a computational approach) is necessary to explicitly give insight into the movement and interaction between molecules and atoms, possibly giving a chance to predict the desulfurization performance.

(8) Despite this promising biomimetic process at the laboratory scale, several key parameters, such as the thermodynamic parameters, energy balance, mass balance, and fluid dynamics are unable to realize the scale-up in practical application. The process simulation is an effective tool to design and optimize this unit operation *via* mathematical model. Thus, DESs-assistant catalytic systems are promising to be practically applicable for the effective desulfurization of fuel oil once the gap between the laboratory and industrialized process is bridged in terms of engineering and technology.

The above biomimetic approach with POMs in DESs is inspirational since biomimetic or bioinspired catalysis is the ''Holy Grail'' of oxidation catalysis. The extraction and oxidation performances of DESs are closely related to the physicochemical properties, which can be tuned by employing various types and molar ratios of HBAs and HBDs. In addition, POMs playing the role of ETMs possess diversities of topology structure and component elements. We are fully convinced that the recent progress made in the field of DESs for the desulfurization will soon definitely open new methodologies for catalytic oxidations, such as the selective oxyfunctionalization of hydrocarbon, in a more rational way.

Conflicts of interest

There are no conflicts to declare.

Acknowledgements

We gratefully acknowledge the financial support from the National Natural Science Foundation of China (No. 22072126, 21925203, 21676230, 21733009 and 21373177) and the Young Scholars Research Fund of Yantai University (No. HY19B26).

References

1 R. T. Yang, A. J. Hernández-Maldonado and F. H. Yang, Desulfurization of transportation fuels with zeolites under ambient conditions, *Science*, 2003, **301**, 79–81.

2 A. J. Hernández-Maldonado and R. T. Yang, Desulfurization of diesel fuels by adsorption via π-complexation with vapor-phase exchanged Cu(I)-Y zeolites, *J. Am. Chem. Soc.*, 2004, **126**, 992–993.

3 T.-M. Chen, W. G. Kuschner, J. Gokhale and S. Shofer, Outdoor air pollution: nitrogen dioxide, sulfurdioxide, and carbon monoxide health effects, *Am. J. Med. Sci.*, 2007, **333**, 249–256.

4 N. Sang, Y. Yun, H. Li, L. Hou, M. Han and G. Li, SO_2 inhalation contributes to the development and progression of ischemic stroke in the brain, *Toxicol. Sci.*, 2010, **114**, 226–236.

5 H. Lü, P. Li, C. Deng, W. Ren, S. Wang, P. Liu and H. Zhang, Deep catalytic oxidative desulfurization (ODS) of dibenzothiophene (DBT) with oxalate-based deep eutectic solvents (DESs), *Chem. Commun.*, 2015, **51**, 10703–10706.

6 G. Lv, S. Deng, Z. Yi, X. Zhang, F. Wang, H. Li and Y. Zhu, One-pot synthesis of framework W-doped TS-1 zeolite with robust Lewis acidity for effective oxidative desulfurization, *Chem. Commun.*, 2019, **55**, 4885–4888.

7 D. Chandran, M. Khalida, R. Walvekar, N. M. Mubarak, S. Dharaskar, W. Y. Wong and T. C. S. M. Gupta, Deep eutectic solvents for extraction-desulphurization: A review, *J. Mol. Liq.*, 2019, **275**, 312–322.

8 P. Tan, Y. Jiang, L. Sun, X. Liu, K. AlBahily, U. Ravon and A. Vinu, Design and fabrication of nanoporous adsorbents for the removal of aromatic sulfur compounds, *J. Mater. Chem. A*, 2018, **6**, 23978–24012.

9 A. Pimerzin, A. Mozhaev, A. Varakin, K. Maslakov and P. Nikulshin, Comparison of citric acid and glycol effects on the state of active phase species and catalytic properties of $CoPMo/Al_2O_3$ hydrotreating catalysts, *Appl. Catal., B*, 2017, **205**, 93–103.

10 R. D. Alli, I. M. AlNashef and M. C. Kroon, Removal of 2- and 3-methylthiophene from their mixtures with n-heptane using tetrahexylammonium bromide-based deep eutectic solvents as extractive desulfurization agents, *J. Chem. Thermodyn.*, 2018, **125**, 172–179.

11 D. Solís, A. L. Agudo, J. Ramírez and T. Klimova, Hydrodesulfurization of hindered dibenzothiophenes on bifunctional NiMo catalysts supported on zeolite–alumina composites, *Catal. Today*, 2006, **116**, 469–477.

12 V. Simanzhenkov and R. Idem, *Crude oil chemistry*, Marcel Dekker, New York, 1st edn, 2003.

13 M. H. Ibrahim, M. Hayyan, M. A. Hashim and A. Hayyan, The role of ionic liquids in desulfurization of fuels: a review, *Renewable Sustainable Energy Rev.*, 2017, **76**, 1534–1549.

14 P. Cruz, E. Granados, M. Fajardo, I. del Hierro and Y. Pérez, Heterogeneous oxidative desulfurization catalysed by titanium grafted mesoporous silica nanoparticles containing tethered hydrophobic ionic liquid: A dual activation mechanism, *Appl. Catal., A*, 2019, **587**, 117241.

15 X. Ma, L. Sun and C. Song, A new approach to deep desulfurization of gasoline, diesel fuel and jet fuel by selective adsorption for ultra-clean fuels and for fuel cell applications, *Catal. Today*, 2002, **77**, 107–116.

16 R. T. Yang, A. J. Hernández-Maldonado and F. H. Yang, New sorbents for desulfurization of liquid fuels by π-complexation, *Ind. Eng. Chem. Res.*, 2001, **40**, 6236–6239.

17 Y. Li, J. Shen, S. Peng, J. Zhang, J. Wu, X. Liu and L. Sun, Enhancing oxidation resistance of Cu(I) by tailoring microenvironment in zeolites for efficient adsorptive desulfurization, *Nat. Commun.*, 2020, **11**, 3206–3214.

18 S. Otsuki, T. Nonaka, N. Takashima, W. Qian, A. Ishihara, T. Imai and T. Kabe, Oxidative desulfurization of light gas oil and vacuum gas oil by oxidation and solvent extraction, *Energy Fuels*, 2000, **14**, 1232–1239.

19 T. Welton, Ionic liquids in catalysis, *Coord. Chem. Rev.*, 2004, **248**, 2459–2477.

20 T. P. T. Pham, C. Cho and Y. Yun, Environmental fate and toxicity of ionic liquids: a review, *Water Res.*, 2010, **44**, 352–372.

21 A. P. Abbott, G. Capper, D. L. Davies, R. K. Rasheed and V. Tambyrajah, Novel solvent properties of choline chloride/urea mixtures, *Chem. Commun.*, 2003, 70–71.

22 A. P. Abbott, D. Boothby, G. Capper, D. L. Davies and R. K. Rasheed, Deep eutectic solvents formed between choline chloride and carboxylic acids: versatile alternatives to ionic liquids, *J. Am. Chem. Soc.*, 2004, **126**, 9142–9147.

23 M. Francisco, A. van den Bruinhorst and M. C. Kroon, Low-transition-temperature mixtures (LTTMs): a new generation of designer solvents, *Angew. Chem., Int. Ed.*, 2013, **52**, 3074–3085.

24 E. L. Smith, A. P. Abbott and K. S. Ryder, Deep eutectic solvents (DESs) and their applications, *Chem. Rev.*, 2014, **114**, 11060–11082.

25 Q. Zhang, K. De Oleveira Vigier, S. Royer and F. Jérôme, Deep eutectic solvents: syntheses, properties and applications, *Chem. Soc. Rev.*, 2012, **41**, 7108–7146.

26 S. E. E. Warrag, C. J. Peters and M. C. Kroon, Deep eutectic solvents for highly efficient separations in oil and gas industries, *Curr. Opin. Green Sust. Chem.*, 2017, **5**, 55–60.

27 M. F. Majid, H. F. M. Zaid, C. F. Kait, K. Jumbri, L. C. Yuan and S. Rajasuriyan, Futuristic advance and perspective of deep eutectic solvent for extractive desulfurization of fuel oil: A review, *J. Mol. Liq.*, 2020, **306**, 112870.

28 N. Guajardo, C. Carlesi, R. Schrebler and J. Morales, Applications of liquid/liquid biphasic oxidations by hydrogen peroxide with ionic liquids or deep eutectic solvents, *ChemPlusChem*, 2017, **82**, 165–176.

29 Y. Liu, J. B. Friesen, J. B. McAlpine, D. C. Lankin, S. Chen and G. F. Pauli, Natural deep eutectic solvents: properties, applications, and perspectives, *J. Nat. Prod.*, 2018, **81**, 679–690.

30 F. Endres, A. Abbott and D. R. MacFarlane, *Electrodeposition from ionic liquids*, John Wiley & Sons, Weinheim, 2nd edn, 2017.

31 C. Florindo, L. C. Branco and I. M. Marrucho, Quest for green-solvent design: from hydrophilic to hydrophobic

(deep) eutectic solvents, *ChemSusChem*, 2019, **12**, 1549–1559.
32 A. P. Abbott, J. C. Barron, K. S. Ryder and D. Wilson, Eutectic-based ionic liquids with metal-containing anions and cations, *Chem. – Eur. J.*, 2007, **13**, 6495–6501.
33 A. P. Abbott, G. Capper, D. L. Davies, H. L. Munro, R. K. Rasheed and V. Tambyrajah, Preparation of novel, moisture-stable, Lewis-acidic ionic liquids containing quaternary ammonium salts with functional side chains, *Chem. Commun.*, 2001, 2010–2011.
34 Y. Feng, M. Li, Z. Gao, X. Zhang, X. Zeng, Y. Sun, X. Tang, T. Lei and L. Lin, Development of betaine-based sustainable catalysts for green conversion of carbohydrates and biomass into 5-hydroxymethylfurfural, *ChemSusChem*, 2019, **12**, 495–502.
35 S. Wang, Z. Zhu, D. Hao, T. Su, C. Len, W. Ren and H. Lü, Synthesis cyclic carbonates with BmimCl-based ternary deep eutectic solvents system, *J. CO2 Util.*, 2020, **40**, 101250.
36 A. P. Abbott, J. C. Barron, K. S. Ryder and D. Wilson, Eutectic-based ionic liquids with metal-containing anions and cations, *Chem. – Eur. J.*, 2007, **13**, 6495–6501.
37 A. P. Abbott, G. Capper, D. L. Davies and R. Rasheed, Ionic liquids based upon metal halide/substituted quaternary ammonium salt mixtures, *Inorg. Chem.*, 2004, **43**, 3447–3452.
38 H. Qin, Z. Song, Q. Zeng, H. Cheng, L. Chen and Z. Qi, Bifunctional imidazole-PTSA deep eutectic solvent for synthesizing long-chain ester IBIBE in reactive extraction, *AIChE J.*, 2019, **65**, 675–683.
39 L. Sun, Z. Zhu, T. Su, W. Liao, D. Hao, Y. Chen, Y. Zhao, W. Ren, H. Ge and H. Lü, Novel acidic eutectic mixture as peroxidase mimetics for oxidative desulfurization of model diesel, *Appl. Catal., B*, 2019, **255**, 117747.
40 A. P. Abbott, G. Frisch, J. Hartley and K. S. Ryder, Processing of metals and metal oxides using ionic liquids, *Green Chem.*, 2011, **13**, 471–481.
41 A. P. Abbott, G. Capper, D. L. Davies, K. J. McKenzie and S. U. Obi, Solubility of metal oxides in deep eutectic solvents based on choline chloride, *J. Chem. Eng. Data*, 2006, **51**, 1280–1282.
42 K. Shahbaz, S. Baroutian, F. S. Mjalli, M. A. Hashim and I. M. AlNashef, Densities of ammonium and phosphonium based deep eutectic solvents: Prediction using artificial intelligence and group contribution techniques, *Thermochim. Acta*, 2012, **527**, 59–66.
43 M. B. Taysun, E. Sert and F. S. Atalay, Effect of hydrogen bond donor on the physical properties of benzyltriethylammonium chloride based deep eutectic solvents and their usage in 2-ethyl-hexyl acetate synthesis as a catalyst, *J. Chem. Eng. Data*, 2017, **62**, 1173–1181.
44 F. Liu, Z. Xue, X. Zhao, H. Mou, J. He and T. Mu, Catalytic deep eutectic solvents for highly efficient conversion of cellulose to gluconic acid with gluconic acid self-precipitation separation, *Chem. Commun.*, 2018, **54**, 6140–6143.
45 Y. Cui, C. Li, J. Yin, S. Li, Y. Jia and M. Bao, Design, synthesis and properties of acidic deep eutectic solvents based on choline chloride, *J. Mol. Liq.*, 2017, **236**, 338–343.
46 A. P. Abbott, G. Capper and S. Gray, Design of improved deep eutectic solvents using hole theory, *ChemPhysChem*, 2006, **7**, 803–806.
47 M. Chi, Z. Zhu, L. Sun, T. Su, W. Liao, C. Deng, Y. Zhao, W. Ren and H. Lü, Construction of biomimetic catalysis system coupling polyoxometalates with deep eutectic solvents for selective aerobic oxidation desulfurization, *Appl. Catal., B*, 2019, **259**, 118089.
48 Y. Hou, Y. Gu, S. Zhang, F. Yang, H. Ding and Y. Shan, Novel binary eutectic mixtures based on imidazole, *J. Mol. Liq.*, 2008, **143**, 154–159.
49 J. Xu, Z. Zhu, T. Su, W. Liao, C. Deng, D. Hao, Y. Zhao, W. Ren and H. Lü, Green aerobic oxidative desulfurization of diesel by constructing an Fe-Anderson type polyoxometalate and benzene sulfonic acid-based deep eutectic solvent biomimetic cycle, *Chin. J. Catal.*, 2020, **41**, 868–876.
50 K. Shahbaz, F. S. Mjalli, M. A. Hashim and I. M. AlNashef, Prediction of deep eutectic solvents densities at different temperatures, *Thermochim. Acta*, 2011, **515**, 67–72.
51 H. Qin, X. Hu, J. Wang, H. Cheng, L. Chen and Z. Qi, Overview of acidic deep eutectic solvents on synthesis, properties and applications, *Green Energy Environ.*, 2020, **5**, 8–21.
52 A. P. Abbott, R. C. Harris, K. S. Ryder, C. D'Agostino, L. F. Gladden and M. D. Mantle, Glycerol eutectics as sustainable solvent systems, *Green Chem.*, 2011, **13**, 82–90.
53 C. Schreiner, S. Zugmann, R. Hartl and H. J. Gores, Fractional Walden rule for ionic liquids: examples from recent measurements and a critique of the so-called ideal KCl line for the Walden plot, *J. Chem. Eng. Data*, 2010, **55**, 1784–1788.
54 M. Hayyan, T. Aissaoui, M. A. Hashim, M. A. AlSasdi and A. Hayyan, Triethylene glycol based deep eutectic solvents and their physical properties, *J. Taiwan Inst. Chem. Eng.*, 2015, **50**, 24–30.
55 C. A. Angell, N. Byrne and J. Belieres, Parallel developments in aprotic and protic ionic liquids: physical chemistry and applications, *Acc. Chem. Res.*, 2007, **40**, 1228–1236.
56 D. J. G. P. van Osch, L. J. B. M. Kollau, A. van den Bruinhorst, S. Asikainen, M. A. A. Rocha and M. C. Kroon, Ionic liquids and deep eutectic solvents for lignocellulosic biomass fractionation, *Phys. Chem. Chem. Phys.*, 2017, **19**, 2636–2665.
57 Y. Loow, E. K. New, G. H. Yang, L. Ang, L. Y. W. Foo and T. Y. Wu, Potential use of deep eutectic solvents to facilitate lignocellulosic biomass utilization and conversion, *Cellulose*, 2017, **24**, 3591–3618.
58 R. Kore and R. Srivastava, Synthesis and applications of novel imidazole and benzimidazole based sulfonic acid group functionalized Brönsted acidic ionic liquid catalysts, *J. Mol. Catal. A: Chem.*, 2011, **345**, 117–126.
59 Y. Yang and Y. Kou, Determination of the Lewis acidity of ionic liquids by means of an IR spectroscopic probe, *Chem. Commun.*, 2004, 226–227.
60 Z. Duan, Y. Gu and Y. Deng, Green and moisture-stable Lewis acidic ionic liquids (choline chloride·x$ZnCl_2$) catalyzed protection of carbonyls at room temperature under solvent-free conditions, *Catal. Commun.*, 2006, **7**, 651–656.

61 M. A. Kareem, F. S. Mjalli, M. A. Hashim and I. M. AlNashef, Phosphonium-based ionic liquids analogues and their physical properties, *J. Chem. Eng. Data*, 2010, **55**, 4632–4637.
62 M. Bengi, T. Emine, S. Ferhan and S. Atalay, Physical properties of benzyl tri-methyl ammonium chloride based deep eutectic solvents and employment as catalyst, *J. Mol. Liq.*, 2016, **223**, 845–852.
63 W. Li, Z. Zhang, B. Han, S. Hu, J. Song, Y. Xie and X. Zhou, Switching the basicity of ionic liquids by CO_2, *Green Chem.*, 2008, **10**, 1142–1145.
64 D. J. G. P. van Osch, J. van Spronsen, A. C. C. Esteves, R. Tuinier and M. Vis, Oil-in-water emulsions based on hydrophobic eutectic systems, *Phys. Chem. Chem. Phys.*, 2020, **22**, 2181–2187.
65 D. J. G. P. van Osch, L. F. Zubeir, A. van den Bruinhorst, M. A. A. Rocha and M. C. Kroon, Hydrophobic deep eutectic solvents as water-immiscible extractants, *Green Chem.*, 2015, **17**, 4518–4521.
66 B. D. Ribeiro, C. Florindo, L. C. Iff, M. A. Z. Coelho and I. M. Marrucho, Menthol-based eutectic mixtures: hydrophobic low viscosity solvents, *ACS Sustainable Chem. Eng.*, 2015, **3**, 2469–2477.
67 C. Florindo, L. G. Celia-Silva, L. F. G. Martins, L. C. Branco and I. M. Marrucho, Supramolecular hydrogel based on a sodium deep eutectic solvent, *Chem. Commun.*, 2018, **54**, 7527–7530.
68 N. Schaeffer, M. A. R. Martins, C. M. S. S. Neves, S. P. Pinho and J. A. P. Coutinho, Sustainable hydrophobic terpene-based eutectic solvents for the extraction and separation of metals, *Chem. Commun.*, 2018, **54**, 8104–8107.
69 C. Florindo, L. Romero, I. Rintoul, L. C. Branco and I. M. Marrucho, From phase change materials to green solvents: hydrophobic low viscous fatty acid–based deep eutectic solvents, *ACS Sustainable Chem. Eng.*, 2018, **6**, 3888–3895.
70 M. A. R. Martins, E. A. Crespo, P. V. A. Pontes, P. V. A. Pontes, L. P. Silva, M. Bülow, G. J. Maximo, E. A. C. Batista, C. Held, S. P. Pinho and J. A. P. Coutinho, Tunable hydrophobic eutectic solvents based on terpenes and monocarboxylic acids, *ACS Sustainable Chem. Eng.*, 2018, **6**, 8836–8846.
71 C. Reichardt, Solvatochromic dyes as solvent polarity indicators, *Chem. Rev.*, 1994, **94**, 2319–2358.
72 M. G. D. Pópolo, J. Kohanoff and R. M. Lynden-Bell, Solvation structure and transport of acidic protons in ionic liquids: A first-principles simulation study, *J. Phys. Chem. B*, 2006, **110**, 8798–8803.
73 G. Law and P. R. Watson, Surface tension measurements of *N*-alkylimidazolium ionic liquids, *Langmuir*, 2001, **17**, 6138–6141.
74 A. P. Abbott, R. C. Harris and K. S. Ryder, Application of hole theory to define ionic liquids by their transport properties, *J. Phys. Chem. B*, 2007, **111**, 4910–4913.
75 C. D'Agostino, M. D. Mantle, L. F. Gladden and G. D. Moggridge, Prediction of mutual diffusion coefficients in non-ideal mixtures from pulsed field gradient NMR data: Triethylamine–water near its consolute point, *Chem. Eng. Sci.*, 2012, **74**, 105–113.
76 R. Häkkinen, O. Alshammari, V. Timmemann, C. D'Agostino and A. Abbott, Nanoscale clustering of alcoholic solutes in deep eutectic solvents studied by nuclear magnetic resonance and dynamic light scattering, *ACS Sustainable Chem. Eng.*, 2019, **7**, 15086–15092.
77 C. D'Agostino, R. C. Harris, A. P. Abbott, L. F. Gladden and M. D. Mantle, Molecular motion and ion diffusion in choline chloride based deep eutectic solvents studied by ^{1}H pulsed field gradient NMR spectroscopy, *Phys. Chem. Chem. Phys.*, 2011, **13**, 21383–21391.
78 I. Delso, C. Lafuente, J. Muñoz-Embid and M. Artal, NMR study of choline chloride-based deep eutectic solvents, *J. Mol. Liq.*, 2019, **290**, 111236.
79 A. P. Abbott, C. D'Agostino, S. J. Davis, L. F. Gladden and M. D. Mantle, Do group 1 metal salts form deep eutectic solvents?, *Phys. Chem. Chem. Phys.*, 2016, **18**, 25528–25537.
80 P. T. Callaghan, *Principles of Nuclear Magnetic Resonance Microscopy*, Oxford University Press, Oxford, 1991.
81 A. Chmielewska and A. Bald, Viscosimetric studies of aqueous solutions of dicarboxylic acids, *J. Mol. Liq.*, 2008, **137**, 116–121.
82 K. Hayamizu, S. Tsuzuki and S. Seki, Molecular motions and ion diffusions of the room-temperature ionic liquid 1,2-dimethyl-3-propylimidazolium bis(trifluoromethylsulfonyl)amide (DMPImTFSA) studied by ^{1}H, ^{13}C, and ^{19}F NMR, *J. Phys. Chem. A*, 2008, **112**, 12027–12036.
83 R. C. Remsing, G. Hernandez, R. P. Swatloski, W. W. Massefski, R. D. Rogers and G. Moyna, Solvation of carbohydrates in N,N-dialkylimidazolium ionic liquids: A multinuclear NMR spectroscopy study, *J. Phys. Chem. B*, 2008, **112**, 11071–11078.
84 S. E. Hooshmand, R. Afshari, D. J. Ramón and R. S. Varma, Deep eutectic solvents: cutting-edge applications in cross-coupling reactions, *Green Chem.*, 2020, **22**, 3668–3692.
85 N. Zec, G. Mangiapia, M. L. Zheludkevich, S. Busch and J. Moulin, Revealing the interfacial nanostructure of a deep eutectic solvent at a solid electrode, *Phys. Chem. Chem. Phys.*, 2020, **22**, 12104–12112.
86 X. Li, J. Choi, W. Ahn and K. H. Row, Preparation and application of porous materials based on deep eutectic solvents, *Crit. Rev. Anal. Chem.*, 2018, **48**, 73–85.
87 A. Abo-Hamad, M. Hayyan, M. A. AlSaadi and M. A. Hashim, Potential applications of deep eutectic solvents in nanotechnology, *Chem. Eng. J.*, 2015, **273**, 551–567.
88 C. Li, D. Li, S. Zou, Z. Li, J. Yin, A. Wang, Y. Cui, Z. Yao and Q. Zhao, Extraction desulfurization process of fuels with ammonium-based deep eutectic solvents, *Green Chem.*, 2013, **15**, 2793–2799.
89 C. Li, J. Zhang, Z. Li, J. Yin, Y. Cui, Y. Liu and G. Yang, Extraction desulfurization of fuels with 'metal ions' based deep eutectic solvents (MDESs), *Green Chem.*, 2016, **18**, 3789–3795.

90 X. Wang, W. Jiang, W. Zhu, H. Li, S. Yin, Y. Chang and H. Li, A simple and cost-effective extractive desulfurization process with novel deep eutectic solvents, *RSC Adv.*, 2016, **6**, 30345–30352.
91 W. Jiang, H. Li, C. Wang, W. Liu, T. Guo, H. Liu, W. Zhu and H. Li, Synthesis of ionic-liquid-based deep eutectic solvents for extractive desulfurization of fuel, *Energy Fuels*, 2016, **30**, 8164–8170.
92 Z. S. Gano, F. S. Mjalli, T. Al-Wahaibi and Y. Al-Wahaibi, The novel application of hydrated metal halide ($SnCl_2 \cdot 2H_2O$)-based deep eutectic solvent for the extractive desulfurization of liquid fuels, *Int. J. Chem. Eng. Appl.*, 2015, **6**, 367–371.
93 W. Jiang, L. Dong, W. Liu, T. Guo, H. Li, S. Yin, W. Zhu and H. Li, Biodegradable choline-like deep eutectic solvents for extractive desulfurization of fuel, *Chem. Eng. Process.*, 2017, **115**, 34–38.
94 J. Li, H. Xiao, X. Tang and M. Zhou, Green carboxylic acid-based deep eutectic solvents as solvents for extractive desulfurization, *Energy Fuels*, 2016, **30**, 5411–5418.
95 X. Tang, Y. Zhang, J. Li, Y. Zhu, D. Qing and Y. Deng, Deep extractive desulfurization with arenium ion deep eutectic solvents, *Ind. Eng. Chem. Res.*, 2015, **54**, 4625–4632.
96 X. Zhao, G. Zhu, L. Jiao, F. Yu and C. Xie, Formation and extractive desulfurization mechanisms of aromatic acid based deep eutectic solvents: an experimental and theoretical study, *Chem. – Eur. J.*, 2018, **24**, 11021–11032.
97 R. Yusof, E. Abdulmalek, K. Sirat and M. B. A. Rahman, Tetrabutylammonium bromide (TBABr)-based deep eutectic solvents (DESs) and their physical properties, *Molecules*, 2014, **19**, 8011–8026.
98 X. Lu, L. Yue, M. Hu, Q. Cao, L. Xu, Y. Guo, S. Hu and W. Fang, Piperazinium-based ionic liquids with lactate anion for extractive desulfurization of fuels, *Energy Fuels*, 2014, **28**, 1774–1780.
99 Z. S. Gano, F. S. Mjalli, T. Al-Wahaibi, Y. Al-Wahaibi and I. M. AlNashef, Extractive desulfurization of liquid fuel with $FeCl_3$-based deep eutectic solvents: experimental design and optimization by central-composite design, *Chem. Eng. Process.*, 2015, **93**, 10–20.
100 A. P. Abbott, K. E. Ttai, G. Frisch, K. J. McKenzie and K. S. Ryder, Electrodeposition of copper composites from deep eutectic solvents based on choline chloride, *Phys. Chem. Chem. Phys.*, 2009, **11**, 4269–4277.
101 Y. Tong Tan, A. S. M. Chua and G. C. Ngoh, Deep eutectic solvent for lignocellulosic biomass fractionation and the subsequent conversion to bio-based products – A review, *Bioresour. Technol.*, 2020, **297**, 122522.
102 L. Hao, M. Wang, W. Shan, C. Deng, W. Ren, Z. Shi and H. Lü, *L*-proline-based deep eutectic solvents (DESs) for deep catalytic oxidative desulfurization (ODS) of diesel, *J. Hazard. Mater.*, 2017, **339**, 216–222.
103 W. Zhu, C. Wang, H. Li, P. Wu, S. Xun, W. Jiang, Z. Chen, Z. Zhao and H. Li, One-pot extraction combined with metal-free photochemical aerobic oxidative desulfurization in deep eutectic solvent, *Green Chem.*, 2015, **17**, 2464–2472.
104 J. Yin, J. Wang, Z. Li, D. Li, G. Yang, Y. Cui, A. Wang and C. Li, Deep desulfurization of fuels based on an oxidation/extraction process with acidic deep eutectic solvents, *Green Chem.*, 2015, **17**, 4552–4559.
105 H. Lü, P. Li, C. Deng, W. Ren, S. Wang, P. Liu and H. Zhang, Deep catalytic oxidative desulfurization (ODS) of dibenzothiophene (DBT) with oxalate-based deep eutectic solvents (DESs), *Chem. Commun.*, 2015, **51**, 10703–10706.
106 D. Hao, L. Hao, C. Deng, W. Ren, C. Guo and H. Lü, Removal of dibenzothiophene from diesels by extraction and catalytic oxidation with acetamide-based deep eutectic solvents, *Chem. Eng. Technol.*, 2019, **42**, 1276–1282.
107 C. Mao, R. Zhao, X. Li and X. Gao, Trifluoromethanesulfonic acid-based DESs as extractants and catalysts for removal of DBT from model oil, *RSC Adv.*, 2017, **7**, 12805–12811.
108 P. Gilli, L. Pretto, V. Bertolasi and G. Gilli, Predicting hydrogen-bond strengths from acid–base molecular properties. The p*K*a slide rule: Toward the solution of a long-lasting problem, *Acc. Chem. Res.*, 2009, **42**, 33–44.
109 L. Hao, T. Su, D. Hao, C. Deng, W. Ren and H. Lü, Oxidative desulfurization of diesel fuel with caprolactam-based acidic deep eutectic solvents: Tailoring the reactivity of DESs by adjusting the composition, *Chin. J. Catal.*, 2018, **39**, 1552–1559.
110 J. M. Campos-Martin, G. Blanco-Brieva and J. L. G. Fierrro, Hydrogen peroxide synthesis: An outlook beyond the anthraquinone process, *Angew. Chem., Int. Ed.*, 2006, **45**, 6962–6984.
111 K. P. Bryliakov, Catalytic asymmetric oxygenations with the environmentally benign oxidants H_2O_2 and O_2, *Chem. Rev.*, 2017, **117**, 11406–11459.
112 J. Piera and J. Bäckvall, Catalytic oxidation of organic substrates by molecular oxygen and hydrogen peroxide by multistep electron transfer—a biomimetic approach, *Angew. Chem., Int. Ed.*, 2008, **47**, 3506–3523.
113 L. Sun, T. Su, J. Xu, D. Hao, W. Liao, Y. Zhao, W. Ren, C. Deng and H. Lü, Aerobic oxidative desulfurization coupling of Co polyanion catalysts and *p*-TsOH-based deep eutectic solvents through a biomimetic approach, *Green Chem.*, 2019, **21**, 2629–2634.
114 Y. Shi, G. Liu, B. Zhang and X. Zhang, Oxidation of refractory sulfur compounds with molecular oxygen over a Ce–Mo–O catalyst, *Green Chem.*, 2016, **18**, 5273–5279.
115 P. Wu, W. Zhu, Y. Chao, J. Zhang, P. Zhang, H. Zhu, C. Li, Z. Chen, H. Li and S. Dai, A template-free solvent-mediated synthesis of high surface area boron nitride nanosheets for aerobic oxidative desulfurization, *Chem. Commun.*, 2016, **52**, 144–147.
116 S. Murata, K. Murata, K. Kidena and M. Nomura, A novel oxidative desulfurization system for diesel fuels with molecular oxygen in the presence of cobalt catalysts and aldehydes, *Energy Fuels*, 2004, **18**, 116–121.
117 J. T. Sampanthar, H. Xiao, J. Dou, T. Y. Nah, X. Rong and W. P. Kwan, A novel oxidative desulfurization process to remove refractory sulfur compounds from diesel fuel, *Appl. Catal., B*, 2006, **63**, 85–93.

118 H. Lü, J. Gao, Z. Jiang, Y. Yang, B. Song and C. Li, Oxidative desulfurization of dibenzothiophene with molecular oxygen using emulsion catalysis, *Chem. Commun.*, 2007, 150–152.

119 L. Gille and H. Nohl, The existence of a lysosomal redox chain and the role of ubiquinone, *Arch. Biochem. Biophys.*, 2000, **375**, 347–354.

120 A. Berkessel, Diversity-based approaches to selective biomimetic oxidation catalysis, *Adv. Inorg. Chem.*, 2006, **58**, 1–28.

121 A. Dolbecq, E. Dumas, C. R. Mayer and P. Mialane, Hybrid organic–inorganic polyoxometalate compounds: from structural diversity to applications, *Chem. Rev.*, 2010, **110**, 6009–6048.

122 N. V. Izarova, M. T. Pope and U. Kortz, Edelmetalle in polyoxometallaten, *Angew. Chem., Int. Ed.*, 2012, **51**, 9492–9510.

123 A. Misra, K. Kozma, C. Streb and M. Nyman, Beyond charge balance: counter-cations in polyoxometalate chemistry, *Angew. Chem., Int. Ed.*, 2019, **59**, 596–612.

124 H. Lü, Y. Zhang, Z. Jiang and C. Li, Aerobic oxidative desulfurization of benzothiophene, dibenzothiophene and 4,6-dimethyldibenzothiophene using an Anderson-type catalyst $[(C_{18}H_{37})_2N(CH_3)_2]_5[IMo_6O_{24}]$, *Green Chem.*, 2010, **12**, 1954–1958.

125 H. Lü, W. Ren, W. Liao, W. Chen, Y. Li and Z. Suo, Aerobic oxidative desulfurization of model diesel using a B-type Anderson catalyst $[(C_{18}H_{37})_2N(CH_3)_2]_3Co(OH)_6Mo_6O_{18}\cdot 3H_2O$, *Appl. Catal., B*, 2013, **138–139**, 79–83.

126 M. Zhang, J. Liu, H. Lia, Y. Wei, Y. Fu, W. Liao, L. Zhu, G. Chen, W. Zhu and H. Li, Tuning the electrophilicity of vanadium-substituted polyoxometalate based ionic liquids for high-efficiency aerobic oxidative desulfurization, *Appl. Catal., B*, 2020, **271**, 118936.

127 X. Wang, Z. Chang, H. Lin, A. Tian, G. Liu and J. Zhang, Assembly and photocatalysis of two novel 3D Anderson-type polyoxometalate-based metal–organic frameworks constructed from isomeric bis(pyridylformyl)piperazine ligands, *Dalton Trans.*, 2014, **43**, 12272–12278.

128 M. Chi, T. Su, L. Sun, Z. Zhu, W. Liao, W. Ren, Y. Zhao and H. Lü, Biomimetic oxygen activation and electron transfer mechanism for oxidative desulfurization, *Appl. Catal., B*, 2020, **275**, 119134.

129 H. Xu, D. Zhang, F. Wu, X. Wei and J. Zhang, Deep desulfurization of fuels with cobalt chloride-choline chloride/polyethylene glycol metal deep eutectic solvents, *Fuel*, 2018, **225**, 104–110.

130 H. Li, J. Wan, Y. Ma, Y. Wang, X. Chen and Z. Guan, Degradation of refractory dibutyl phthalate by peroxymonosulfate activated with novel catalysts cobalt metal-organic frameworks: Mechanism, performance, and stability, *J. Hazard. Mater.*, 2016, **318**, 154–163.